Actuation for flexible and stretchable microdevices

Uditha Roshan, [a] Amith Mudugamuwa, [a] Haotian Cha,[a]
Samith Hettiarachchi, [a] Jun Zhang [*ab] and Nam-Trung Nguyen [*a]

Flexible and stretchable microdevices incorporate highly deformable structures, facilitating precise functionality at the micro- and millimetre scale. Flexible microdevices have showcased extensive utility in the fields of biomedicine, microfluidics, and soft robotics. Actuation plays a critical role in transforming energy between different forms, ensuring the effective operation of devices. However, when it comes to actuating flexible microdevices at the small millimetre or even microscale, translating actuation mechanisms from conventional rigid large-scale devices is not straightforward. The recent development of actuation mechanisms leverages the benefits of device flexibility, particularly in transforming conventional actuation concepts into more efficient approaches for flexible devices. Despite many reviews on soft robotics, flexible electronics, and flexible microfluidics, a specific and systematic review of the actuation mechanisms for flexible and stretchable microdevices is still lacking. Therefore, the present review aims to address this gap by providing a comprehensive overview of state-of-the-art actuation mechanisms for flexible and stretchable microdevices. We elaborate on the different actuation mechanisms based on fluid pressure, electric, magnetic, mechanical, and chemical sources, thoroughly examining and comparing the structure designs, characteristics, performance, advantages, and drawbacks of these diverse actuation mechanisms. Furthermore, the review explores the pivotal role of materials and fabrication techniques in the development of flexible and stretchable microdevices. Finally, we summarise the applications of these devices in biomedicine and soft robotics and provide perspectives on current and future research.

[a] Queensland Micro and Nanotechnology Centre, Griffith University, Brisbane, QLD 4111, Australia. E-mail: nam-trung.nguyen@griffith.edu.au, jun.zhang@griffith.edu.au
[b] School of Engineering and Built Environment, Griffith University, Brisbane, QLD 4111, Australia

Uditha Roshan

Uditha Roshan received his Bachelor of the Science of Engineering Honours and the Master of Philosophy degrees in Mechanical Engineering from the University of Moratuwa, Sri Lanka in 2016 and 2022 respectively. He started his doctoral studies in 2023 and is currently a Ph.D. candidate at Queensland Micro- and Nanotechnology Centre (QMNC), Griffith University, Australia. His research focuses on design and development of microelastofluidic systems for biomedical applications. His research interests are microfluidics, microelastofluidics, smart material-based actuation, and micro/ nano-electromechanical systems (MEMS/NEMS).

Amith Mudugamuwa

Amith Mudugamuwa received his bachelor's degree in mechanical engineering from the University of Moratuwa (UOM), Sri Lanka in 2017. He received his MPhil. in mechatronic engineering from Shandong University of Science and Technology (SDUST), China in 2020. He is currently a PhD candidate at Queensland Micro- and Nanotechnology Centre (QMNC), Griffith University, Australia. His current research focuses on innovative inertial microfluidics for micro/nano particle manipulation. His research interests include microfluidics, lab-on-a-chip, micro/nano- electromechanical systems (MEMS/NEMS), computer vision, vibration-based sensing, and artificial intelligence.

1. Introduction

Over the past decades, device miniaturisation, flexibility, and stretchability have received increasing attention to enhance portability and wearability, overcome dimensional constraints and functionality limitations, improve conformability on complex and curved body surfaces, and achieve long-term stability and reliability.[1] These superior properties can enable broad applications of flexible and stretchable microdevices on electronic skin,[2] smart fabric,[3] wearable energy harvesters,[4] wireless communication devices,[5] emerging displays,[6] etc.

Flexible and stretchable microdevices consist of highly deformable structures capable of precise micro and millimetre scale deformation. Accurate, adaptable, and versatile actuation is critical to control the device structures and fulfil the functionality of flexible microdevices.

Actuation is the principle and mechanism to translate the energy of various formats into the mechanical motion of devices or device components for specific functions and tasks.[7] The energy can be from mechanical, pneumatic, hydraulic, electrical, thermal, magnetic, and chemical sources.[8] Many actuation mechanisms have been well developed for

Haotian Cha received his bachelor's degree in engineering from Nanjing University of Science and Technology (NUST) and master's degree in engineering from the University of New South Wales (UNSW). He currently holds a position as a Ph.D. candidate in Queensland Micro and Nanotechnology Centre (QMNC) at Griffith University, Australia. His leading research focuses on developing innovative Multiphysics

Haotian Cha

Microfluidics technology, especially inertial microfluidic technology for flexible cell focusing and separation. His research interests include dielectrophoresis (DEP), hydrophoresis, inertial microfluidic technology, and the development of lab-on-a-chip biomedical applications.

Samith Hettiarachchi received his honours degree in engineering (mechanical engineering) from the University of Moratuwa, Sri Lanka. He is currently a Ph.D candidate at Queensland Micro- and Nanotechnology Centre (QMNC), Griffith University, Australia. His research focuses on developing mechanisms for submicron to nanoparticle manipulation, focusing, and separation using microfluidics. His research interests are

Samith Hettiarachchi

microfluidics, lab-on-a-chip, inertial microfluidics, viscoelastic microfluidics and computational fluid dynamics.

Jun Zhang is a Senior Lecturer at the School of Engineering and Built Environment, Griffith University, Australia. He was a recipient of an ARC DECRA fellowship (2021–23). He received his bachelor's degree in engineering with an Outstanding Graduate Award from the Nanjing University of Science and Technology (NUST), China, in 2009, and received a PhD degree in Mechanical Engineering from the University of

Jun Zhang

Wollongong, Australia, in 2015. His research is to explore the passive fluid dynamics, active external (electrical, acoustic, magnetic etc.) force fields and their combination to accurately manipulate micro- and nanoparticles in rigid and flexible microfluidic platforms, as well as develop microfluidic technologies for disease diagnosis and therapeutics.

Nam-Trung Nguyen is an Australian Laureate Fellow. He received his Dipl-Ing, Dr Ing, and Dr Ing Habil degrees from Chemnitz University of Technology, Germany, in 1993, 1997, and 2004, respectively. From 1999 to 2013, he was an Associate Professor at Nanyang Technological University in Singapore. Since 2013, he has served as a Professor and the Director of Queensland Micro- and Nanotechnology Centre of

Nam-Trung Nguyen

Griffith University, Australia. He is a Fellow of ASME and a Senior Member of IEEE. His research is focused on microfluidics, nanofluidics, micro/nanomachining technologies, micro/nanoscale science, and instrumentation for biomedical applications. One of his current research interests is developing flexible and stretchable systems with bio interface.

conventional macroscale rigid devices and machines such as automotive, aircraft, robotics, *etc.*[9-11] For example, direct mechanical actuation converts one type of mechanical motion into another using machine elements such as levers, pulleys, gears, and linkages in robotics.[7] Pneumatic and hydraulic actuation uses the potential energy of compressed gas and liquid to tune the flight control surfaces of aeroplane wings and the motion of the aeroplane.[12] Electric actuators such as electric motors convert electrical energy into mechanical motion. Thermal actuators attached to the chevrons on the tailing edges of jet engines, change shape absorbing the thermal energy from the combusted air to improve their acoustic performance.[13,14] Magnetic actuation is used in proportional pressure control valves in automobile antiskid braking systems to control the braking force precisely.[15] Chemical actuators convert chemical energy into mechanical energy by combustion that facilitates movement in petrol car engines.[16] These actuation mechanisms have achieved great success and are widely used in everyday life.

However, the actuation mechanisms for the conventional rigid and large devices cannot be straightforwardly translated to flexible microdevices on the small millimetre or even microscale. There are many limitations, such as reduced efficiency, domination of surface effects at the microscale, and manufacturability for scaling down conventional actuation concepts from macro to microdomain.[17-19] Therefore, dedicated actuation mechanisms, novel materials, and advanced fabrication techniques are under development to address these issues.[20-27] For example, it is impossible to apply conventional electromagnetic motor-based actuation for microrobots used for targeted drug therapy for minimally invasive medicine because of the limited miniaturisation capability of the electromagnetic motors. Instead, microactuator structures such as helical propellers made of magnetic materials have been developed to navigate microrobots through external magnetic fields.[28] In addition, highly complex and dynamic environments demand microdevices with high flexibility, dexterity, and efficient force transmission in minimally invasive surgeries.[29] Conventional materials cannot satisfy all these requirements, and advanced materials such as shape memory alloy (SMA) have been developed for highly dexterous, miniaturised flexible devices.[30]

Flexible devices have broad applications in biomedical technology, microfluidics, and soft robotics. Wearable and implantable devices in biomedical applications require microdevices to conform to the human body for real-time diagnosis and treatments.[31] Therefore, the actuator structures inside the device must be highly flexible and stretchable for comfortable attachment to the body.[32] Besides, fluid manipulation at the microscale through microvalves and micropumps is facilitated by pneumatically or hydraulically deforming flexible and stretchable microstructures.[33-35] Soft robotics emulates the dexterity and compliance of natural organisms, enables safe navigation in complex and dynamic environments, and minimally invasive surgery.[36-38] Although there are many reviews on soft robotics,[39] flexible electronics,[40] and flexible microfluidics,[34] a specific and systematic review of the actuation mechanisms for flexible and stretchable microdevices is still lacking.

This paper aims to systematically review the state-of-art actuation mechanisms for flexible and stretchable microdevices. We first elaborate on the fundamental working principle of different actuation mechanisms based on power sources of pneumatic,[41] hydraulic,[36] thermal,[42] electrical,[43] magnetic,[44] humidity,[45] chemical,[46] mechanical,[47] *etc.* The structure designs, characteristics, and performance of various actuators are discussed and compared. Next, we discuss the materials and fabrication techniques for developing flexible actuators and devices. After that, we summarise several typical applications of flexible actuation, such as microscale fluid handling, tissue engineering, organ-on-a-chip, and soft robotics (Fig. 1). Finally, we discuss current challenges and provide future perspectives on the actuation of flexible and stretchable microdevices.

2. Actuation principles

Many actuation mechanisms have been developed based on various energy sources such as fluidic pressure, electric, thermal, magnetic, chemical, *etc.* This chapter aims to familiarise the readers with the general actuation concepts, working principles, typical design features, and actuation performance. In addition, this section emphasises the relevance of these actuation mechanisms for flexible and stretchable devices, especially from recently reported works, but does not exhaustively discuss all the actuation mechanisms.

2.1. Fluid-driven actuation

Fluid-driven actuation relies on the deformation or displacement of one or more boundaries of an enclosed chamber due to the fluid pressure.[48] Compressed,[49] vacuumed,[50] or a combination of compressed and vacuumed[51,52] fluids can be the driving source for the deformation or displacement of the flexible boundaries. Both liquid and gas can serve as the working mediums.[36,53-55] Fluid-driven actuation can be further classified as hydraulic and pneumatic actuation. In the following section, we will briefly describe the typical design of hydraulic and pneumatic actuators and discuss their characteristics and performance. Table 1 summarises and compares parameters related to the design, fabrication and performance of some reported fluid-driven actuators.

Pneumatic microactuators have a flexible structure that can deform under pressure or vacuum, Fig. 2A. The flexible element can be a flat membrane made of a flexible material,[56,57] or a flexible chamber.[58] These flexible structures have been widely used in pneumatic micropumps[51,53,54,59-62] and microvalves.[52,56-58,63,64] The flexible membranes used in microvalves and micropumps can be circular,[52] rectangular,[64] or any other shape, depending on the enclosed microchannels. Also, the cross-sectional shape of the membrane is a decisive factor in accurately dispensing small fluid volumes through pneumatic micropumps. A flat, membrane creates a considerable dead volume, reducing the pumping efficiency. In contrast, arched
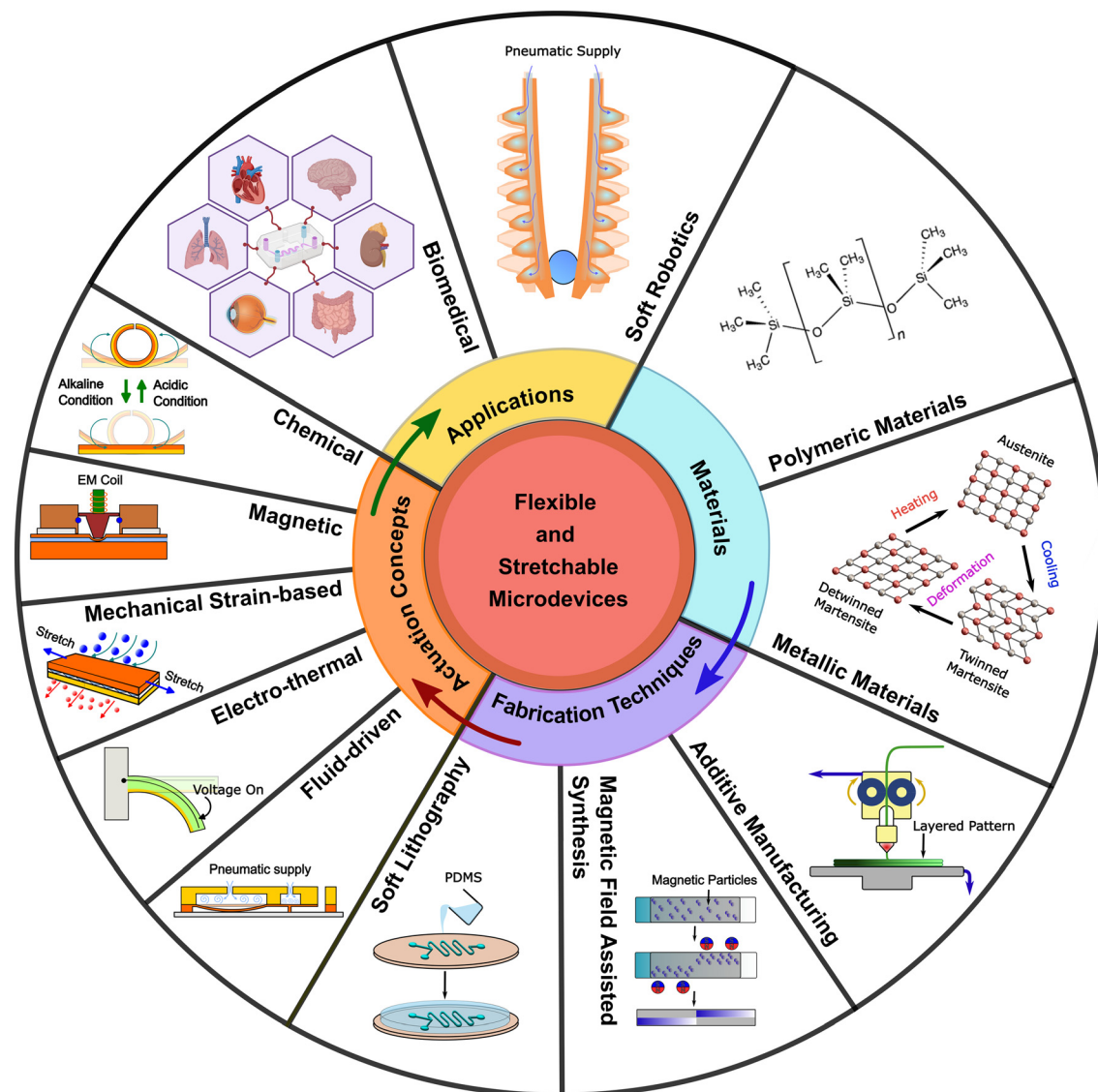
Fig. 1 A schematic overview of actuation mechanisms, device materials, fabrication techniques, and applications for flexible and stretchable microdevices.

membranes[60] can reduce the dead volume and improve the pumping efficiency. However, small clearances[56] between the flexible membrane and the sealing surface are also a solution for enhancing pumping efficiency. Furthermore, the flexible structure not only serves as a valve to fully close a microchannel in microvalves but also acts as a regulator by partially closing the microchannel to tune its fluidic resistance.[64]

The performance of pneumatic actuators in micropumps and microvalves depends on many parameters. The thickness of the flexible membrane is the key parameter. For the same surface area, a thicker membrane requires a higher pressure to achieve valving and pumping functions.[53] Next, the pumping rate in a micropump is greatly affected by parameters such as the membrane elasticity,[59] the time taken to release the pressurised air,[59,60] or the applied negative pressure.[59] Moreover, the flow rate also depends on the pumping frequency. The pumping frequencies reported in

the literature range from 1 to 40 Hz, and the flow rate of micropumps is pL min^{-1} to mL min^{-1}.[51,53,54,59–62] Theoretically, a high pumping frequency can obtain a higher flow rate.[65] Nevertheless, this is only true for the frequency below the first resonant frequency of the pumping membrane. The flow rate may decrease monotonically with increasing frequency after reaching a peak.[54] Depending on the dynamic behaviour of the system, pumping can either be unidirectional or bi-directional.[66]

Hydraulic microactuators use flexible structures that deform under pressurised liquid to facilitate actuation. These flexible elements include membranes,[67] flexible chamber structures like bellows,[68] soft tubular structures,[36] Fig. 2B, or artificial tentacles.[69] These flexible elements have been used in transportation units,[55] micropumps,[36] and microvalves.[67] In addition, some bio-inspired flexible actuators[68–70] were also designed based on this actuation principle. For a given

Table 1 Fluid-driven actuation principles

Actuation	Actuator type	Dimensions	Material(s)	Fabrication method(s)	Pressure input (kPa)	Mode of actuation	Max. Flow rate (μL min^{-1})	Force	Application(s)	Ref.
Pneumatic	Micro pumps	D – 2 mm T – 200 μm	PMMA, PDMS	Micromachining (pneumatic and fluidic layers) with oxygen plasma bonding	300 (air)	Peristaltic	1633	NA	Blood plasma extraction	53
		D – 5.2 mm T – 250 μm	Glass, PDMS	Soft lithography with oxygen plasma bonding	(−)39.9 (vacuum), 13.8 (air)	Reciprocating	360	NA	Detection of NT-proBNP biomarker	59
		D – 2 mm T – 25 μm	PMMA, TPU	Laser machining with thermal fusion bonding	70 (N$_2$)	Peristaltic	3.5	NA	Cell culture	54
		L – 200 μm W – 200 μm T – 20 μm	Glass, PDMS	Soft lithography with oxygen plasma bonding	100 (N$_2$)	Peristaltic	0.026	NA	Heart/cancer on a chip	61
		T – 250 μm	Glass, PDMS	Soft lithography with oxygen plasma bonding	(−)40 (vacuum), 6.8 (air)	Reciprocating	1999	NA	Aptamer identification	62
	Micro valves	L – 1.5 mm W – 500 μm T – 150 μm	Glass, PDMS	Soft lithography with oxygen plasma bonding	172.4 (air), Vacuum	Reciprocating (on–off)	NA	NA	Aptamer-affinity separation	52
		L – 200 μm W – 50 μm T – 10 μm	Glass, PDMS	Soft lithography with oxygen plasma bonding	~71 (air)	Reciprocating (on–off)	NA	NA	Single-cell sorting	63
		L – 10 mm W – 5 mm	PDMS	3D printing and sacrificial manufacturing technique	15 (air)	Simultaneous squeez/release (on–off)	NA	NA	Analysis of enzyme kinetics	58
		L – 300 μm W – 50 μm T – 20 μm	Glass, PDMS	Soft lithography with oxygen plasma bonding	200 (air)	Reciprocating (flow controlling)	1.3	NA	Generation of dynamic concentration of diffusible molecules	64
Hydraulic	Micro pumps	L – 5 mm W – 2 mm T – 120 μm	PDMS	PDMS replica moulding with oxygen plasma bonding	(Ionic liquid)	Peristaltic	5	NA	Compact fluid delivery systems	67
	Bellows	D – 50 μm T – 1 μm V – 4.9 × 10^{-4} mm^3	IP-DIP resin	2PP 3D printing	31 (uncured IP-DIP)	Compression	NA	200–300 μN	Soft robotics	68
	Muscle	L – 235 mm D – 3.18 mm	TPU, Ecoflex™, yarn	3D printing, soft moulding	ΔP = −1500 (water)	Expansion and contraction	174 × 10^3	34.2 N	Robotics and medical	36

L – length; W – width; T – thickness; D – diameter; V – volume.

design, the applied liquid pressure is the main parameter for the output displacement.[70] Cheng et al.[69] showed that increasing the injected water volume from 0.7 to 1.25 mL in their hydraulic actuator caused a curvature change from 18 to 42.6 m^{-1}. The working liquid of hydraulic microactuators is generally supplied externally. Still, there are instances where the working liquid is already enclosed in the actuation chamber during the fabrication process, eliminating the requirement for external sources.[68]

Hydraulic actuators have great potential in microscale applications,[71] such as transmitting high forces and creating three-dimensional motions.[68] Hydraulic actuation also
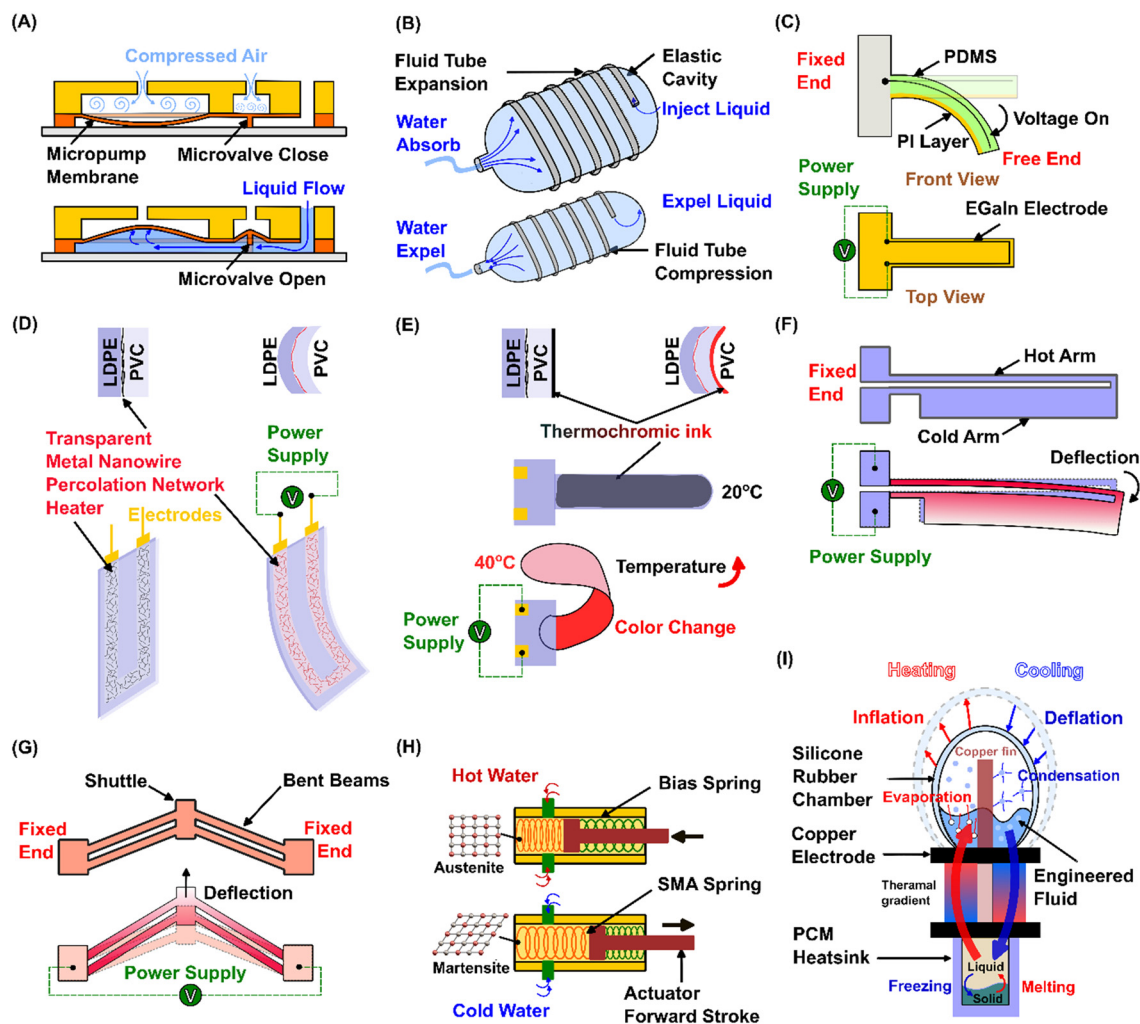
Fig. 2 Actuation schemes. (A) Microfluidic pumps and valves operated by compressed air and vacuum.[51] (B) A micropump works by expansion and contraction of a tubular structure and bi-directional fluid flow.[36] (C) A non-metallic bi-morph actuator embedded with an eutectic GaIn heater.[72] (D) An anisotropic transparent shape morphing actuator consists of transparent silver nanowire (AgNW) percolation network as the heating element.[73] (E) A color-changing electro-thermal actuator consists of thermochromic pigments coated on the passive layer.[74] (F) A hot and cold arm electro-thermal actuator deflects under an applied electric voltage. (G) A bent-beam electro-thermal actuator diverts under an applied voltage. (H) A shape memory alloy (SMA) linear actuator retracts and extends under the temperature-induced phase change of spring-type element.[75] (I) A soft-thermo-pneumatic actuating module consists of thermoelectric element facilitating actuation cycles.[76]

provides more portability than pneumatic actuation in some environments.[68] Because the working liquid of the hydraulic actuators can be stored within the actuator structures eliminating external reservoirs and making actuators more portable. Besides, the working liquid and the materials of the flexible structures in hydraulic actuators play important roles in their performance. For example, the working liquid for self-containing hydraulic microactuators must be carefully selected to minimise viscosity variations, evaporation, and hygroscopic nature that would affect long-term performance. Speller *et al.*[67] developed a self-contained hydraulically-actuated microfluidic (SCHAM) device that uses 1-methyl-3-butylimidizaolium-based ionic liquids as the working liquid. The team demonstrated that the ionic liquid-based SCHAM performs better than the water-based counterparts because of less change in fluidic mass due to evaporation. In addition,

the viscosity of the working fluid is a significant factor because higher viscosities cause slow response and hysteresis. For example, a fully enclosed hydraulic microactuator that uses uncured IP-DIP (Nanoscribe GmbH) (dynamic viscosity, $\mu = 2420$ mPa s) resins as the working fluid shows less efficient and slower response than IP-PDMS (Nanoscribe GmbH) ($\mu = 2$ mPa s) resins.[68]

In summary, fluid-driven actuation has the advantages of reliability, fast operation, scalability, and contamination-free operation. However, limitations exist, such as the need for external pressure or vacuum sources and leakproof designs, making fluid-driven actuators more bulky than other schemes. Compared to pneumatic actuation, hydraulic actuation provides higher power density with promising performance in the microscale,[68] particularly in soft robotics. Overall, the low compressibility of liquids compared to gases

makes hydraulic actuation more precise than its pneumatic counterparts.

2.2. Electro-thermal actuation

Electro-thermal actuators operate based on Joule heating and the associated thermal effect in actuator materials. The temperature increase causes the materials to deform due to thermal expansion or phase change, performing actuation tasks. Therefore, electro-thermal actuation mainly consists of thermal expansion and phase change mechanisms. Structure designs based on the thermal expansion mechanism include bi-morph,[77] hot and cold arms,[78] and bent-beam.[79] The phase change mechanism has been applied in smart material actuation,[75,80] and thermo-pneumatic actuation.[81] Table 2 summarises and compares critical parameters (e.g., maximum deformation, temperature, and voltage), fabrication methods, and applications of some reported electro-thermal actuators.

Thermal expansion-based actuators undergo deformation according to temperature changes. The following equation describes the length change of material under increasing temperatures,

$$L - L_0 = L_0 \alpha \Delta T \qquad (1)$$

where L and L_0 are the final and initial lengths of the materials, and α and ΔT are the coefficient of thermal expansion (CTE) of the material and the temperature difference, respectively. Applying an electric current across the material causes joule heating and increases in the temperature. The temperature increase results in the expansion of the materials.

Bimorph microactuators consist of two layers of materials with different CTEs bonded together, Fig. 2C. The temperature increase results in thermal expansion in both material layers, but the mismatched thermal expansion coefficients cause the deflection to be orders of magnitude higher than the intrinsic expansion. According to eqn (1), parameters such as L_0 and ΔT are the same for the two layers, but the layer with higher CTE elongates more than the layer with lower CTE. Since the two layers are bonded, the bimorph structure bends toward the layer with the lowest CTE,[82] resulting in actuation stroke and force. Bi-morph actuators are classified into in-plane, out-of-plane,[72,83,84] two-dimensional (2D) spiral,[77] and three-dimensional (3D) spiral[85] according to their spatial motion. The most recent advancements of bi-morph actuators are the transparent electro-thermal,[86] Fig. 2D, and color-changing electro-thermal,[74] Fig. 2E, as well as actuators that are categorised based on the visual appearance. The transparent electro-thermal actuators consist of transparent thermoresponsive layers and a heating layer. This brings the advantage of optical transparency to the actuators. Ko et al.[86] reported a shape-morphing transparent electro-thermal actuator made of low-density polyethylene (LDPE) and polyvinyl chloride (PVC) as thermoresponsive layers and highly transparent

Table 2 Electro-thermal actuation principles

Actuation	Actuator type	Dimensions	Material(s)	Fabrication method(s)	Voltage (V)	Temp. (°C)	Mode of actuation	Max. Deformation/speed	Force	Application(s)	Ref.
Thermal expansion	Bi-morph	L – ~800 μm, ~1500 μm	NiTiNOL-Al nanofilms	MEMS manufacturing methods	0–2.5	52	Out-of-plane	Linear – 2.96 mm s⁻¹ Angular – 167° s⁻¹	NA	Biomedicine, microrobots	83
		L/W: 8:1 T – ratio: 10:1 (PDMS:PI)	PDMS-EGaIn-PI	3D printing (EGaIn), spin coating (PDMS)	0.5–3	119	Out-of-plane	Angular – 116°	11.2 mN	Bionic soft robots	72
		A – (IP-S: 2050 Galinstan: 2500) μm²	(IP-S)-Galinstan-(IP-S)	TPP 4D printing, liquid metal microfluidic injection	0.386	62	3D rotary-spiral	Angular – 10°	NA	Soft microrobots	85
		T – PDMS: 200 μm PI: 40 μm, 50 μm	PI-LIG-PDMS	Direct laser scanning (LIG on PI), spin coating (PDMS)	30	93.7	2D rotary-spiral	Angular – 1080°	110 × actuator weight	Reconfigurable 3D assembly, human-soft actuator interaction, artificial muscles.	77

Table 2 *(continued)*

Actuation	Actuator type	Dimensions	Material(s)	Fabrication method(s)	Voltage (V)	Temp. (°C)	Mode of actuation	Max. Deformation/speed	Force	Application(s)	Ref.
		L – 10–20 mm T – PDMS: 50–150 µm Graphene: 25 µm	Graphene–PDMS	Spin coating (PDMS), adhesion (graphene on PDMS)	0–10 pulses	98	Out-of-plane	Linear – 6.89 mm s^{-1}	~0.12 mN	MEMS, artificial muscles, switches	84
	Hot-cold arm	Hot arm L – 1000 µm Cold arm L – 850 µm Hot arm W – 10 µm Cold arm W – 50 µm T – 50 µm	Silicon-on-insulator (SOI)	Integrated circuit fabrication process	NA	278	In-plane	9.45 µm	~0.14 mN	Microgripper	96
	Bent beam	Primary beam W – 6 µm Secondary beam W – 6.6 µm T – SOI: 25 µm Angle: 7°	Silicon-on-insulator (SOI)	SOIMUMPs™26 micromachining	5	86.4	In-plane	26.3 µm	NA	Human RBC characterisation	103
		Beam L – 303 µm Beam W – 20 µm T – Al: 2 µm Angle: 2°	Aluminum	Surface micromachining	0–1	201	In-plane	11 µm	NA	Micro-object manipulation	79
		Beam L – 3100 µm Beam W – 50 µm T – SOI: 125 µm Angle: 1°	Silicon-on-insulator (SOI)-Au	Double-sided etching process with an inductively coupled plasma (ICP) technique	4	NA	In-plane	80.75 µm	NA	Actuators in miniature mechatronic systems	101
Phase change	Thermo-pneumatic	Bellows V – 26.4 mm³	PDMS	3D printed soluble melding technique	0.55	492	Out-of-plane	2.184 mm	90.2 mN	Soft micro-robots	81
	SMM	PE flat wire A – 0.05 mm² SME wire D – 100 µm	NiTiNOL	Commercially SMA wires combined with 3D-printed structures	5.4	73	Out-of-plane	0.8 mm	20 kPa holding pressure	Microvalves, micropumps	80

L – length; W – width; T – thickness; D – diameter; A – cross-sectional area; V – volume.

silver nanowire (AgNW) as the resistive heating element. This actuator showed a bending curvature >2.5 cm^{-1} at 40 °C. In addition, the team also applied thermochromic pigments on the surface of the transparent actuator structure that allows intuitive color changes depending on the temperature, resulting in color change electro-thermal actuators.[74] The performance of bi-morph actuators can be improved by altering the thickness ratio of the material layers. Ultra-thin structures[83,87] improve the dynamic characteristics of the microactuators because of fast heating and cooling rates due to the high surface-to-volume ratio. A recent study showed that a bi-morph electro-thermal microactuator consisting of layers with thicknesses from 400 to 500 nm could undergo precise and rapid actuation (up to 100 Hz) within a temperature bandwidth of less than 52 °C.[83] However, combining materials such as LDPE and PVC that show high directional (anisotropic) and isotropic thermomechanical behaviours respectively provides bimorph actuators with large CTE mismatch, enabling large deformations.[86] Also, liquid metals such as eutectic GaIn (EGaIn),[72] and Galinstan[85] as the conductive paths can improve resistance stability and rapid heating of the bi-layers. Furthermore, the transparent AgNW percolation networks[86] used in electrothermal actuators improve the transparency of the actuators while serving as the conductive path. Laser-induced graphene (LIG) used for the conductive layers of a bi-morph actuator can serve as a sensor, where the deformation of LIG causes a resistance change.[88] Compared to other thermal expansion-based actuator types, bi-morph actuators can produce precise and fast actuation tasks in the microscale.

The pseudo-bimorph thermal actuator,[89] also known as a hot and cold arm or folded beam actuator, consists of two arms connected in a series, Fig. 2F. In this configuration, both arms are made of the same material. Differences in parameters such as length,[90] cross-section,[91] and doping levels[92] of the two arms lead to a mismatch in resistance, causing an asymmetrical temperature distribution between the hot and cold arms. As a result, dissimilar expansion causes the connected beams to bend toward the cold arm. Multiple hot arms were used to improve the performance of this actuator.[93] Structural design optimisation could improve the bending displacement of a pseudo-bi-morph actuator.[94] This type of actuator can also provide both in-plane[94] and out-of-plane[95] motions. The actuation performance of pseudo-bi-morph actuators primarily depends on the temperature difference between the hot and cold arms. A higher temperature difference can be achieved by removing the excess heat generated at the hot arm. Zhang et al.[96] used a fin structure connected to the hot arm in their microgripper design, improving the excess heat dissipation. This results in increased temperature difference, providing higher displacement of the actuator.

The V-shape or chevron-type actuators, also known as bent-beam actuators,[97] work based on linear thermal expansion similar to the above actuators. A bent-beam actuator has a planar configuration where two planar arms are anchored at opposite ends, and the other ends are connected with a common point known as a shuttle, Fig. 2G. The In-plane displacement of the bent-beam actuator can be obtained by a coupled thermo-mechanical mechanism.[98,99] Geometrical parameters, such as the initial beam inclinations, lengths, and the location of the fixed ends of the beams, determine the motion of the shuttle.[100] Higher inclination angles cause adverse effects on the effective displacements. Therefore, inclination angles should be as low as possible to achieve higher in-plane displacements. For instance, Dai et al.[101] chose 1⁰ inclination angles for the designed bent-beam actuator and achieved 80.75 μm in-plane displacement with a 4 V input voltage. The configurations of bent-beam actuators include beam-array,[102] cascaded bent-beam,[103] Z-shape beam,[100] and out-of-plane bent-beam.[104] Moreover, bent-beam type actuators can be improved by carefully selecting the number of beams to provide higher displacements while improving the mechanical performance.[103] The main reason for the improved performance is the close arrangement of beams that isolate the actuator from its surroundings, resulting in a higher operating temperature. The bent-beam actuator configuration is more robust than other electro-thermal actuators.

Electro-thermal actuators based on phase change convert input energy to work through the change in the material phase.[105] Once mechanically deformed, smart materials such as shape memory alloys change crystal structure and return to undeformed shape (shape memory effect) upon altering the temperature,[75] Fig. 2H. This phenomenon is known as solid–solid phase transformation or crystallographic transformation.[80] In addition, thermo-pneumatic actuation uses the expansion of gas,[81] or a change in the volume of liquid or solid in a confined space under heat input.[106] The phase change happens with liquid evaporating into gas[76,107] or solid melting into liquid, resulting in considerable volume expansion. This phenomenon increases pressure to deflect the flexible walls of the confined space and do external work on the environment. The actuating flexible structures can be in the form of membranes,[108] inflatable chambers,[76,107] or bellows,[81] where the surrounding walls deflect to create the actuation. Yoon et al.[76] reported a phase change soft actuator capable of bi-directional operation by thermoelectric heating and cooling. They used Novec™ 7100 Engineered Fluid (Sigma-Aldrich, SHH0002) with a boiling point of 61 °C as the working medium inside the inflatable chamber. Thermoelectric heating changed the phase of the fluid from liquid to gas, which enhances the pressure and induces inflation. In contrast, thermoelectric cooling changes the phase of the evaporated gas to liquid, decreasing the pressure and resulting in deflation, Fig. 2I.

2.3. Magnetic actuation

Magnetic actuators use the potential energy of the magnetic fields to produce mechanical motion.[109] The working principles of magnetic actuators are based on permanent magnets,[110]

electromagnets,[111,112] magnetorheological fluid,[113] magnetic hydrogel,[44] magnetic shape memory materials,[114] and magnetostriction.[115] Among these schemes, the most straightforward is utilising attractive and repulsive forces between permanent magnets. On the other hand, the force generated on a ferromagnetic core by current-carrying coils or a current-carrying conductor in a magnetic field is used in electromagnetic actuation. Moreover, magnetorheological fluids are magnetic particle suspensions, and their fluid properties depend on the magnetic field. Varying a magnetic field causes magnetic shape memory materials to shift between different material structures and enable actuation. Magnetostrictive materials are ferromagnetic and undergo strains when subjected to magnetic fields. Table 3 summarises and compares parameters related to the design, fabrication and performance of some reported magnetic actuators.

Magnetic microactuators also utilise membranes[111,112,116] and flexible structures[113,117,118] for actuation purposes. Attractive and repulsive forces generated by an electromagnetic coil deflect the flexible membranes attached to permanent magnets.[112] For example, Liu et al.[116] developed a normally closed microvalve using an electromagnetic coil surrounding a ferromagnetic core, Fig. 3A. Initially, the flexible membrane attached to the core deflects under an extension of an external spring and closes the microchannel. The valve opens by recovering the membrane deflection as the electromagnet is energised to contract the external spring. In this work, the membrane thickness is an important parameter that dictates the magnetic force required to deflect the membrane for the actuation.

Liquid metal microfluidic networks embedded in elastomer matrix membranes can be used for unique actuation tasks where Lorentz forces can locally deform the membranes.[111] Lorentz forces act on the liquid metal channel as the current passes through it, locally deforming the membrane, Fig. 3B. The electric current and magnetic flux density determine the magnitude of the Lorentz force and, in turn, the membrane deflection. The performance of flexible actuators developed by embedding liquid metal layers in elastomeric membranes significantly depends on the viscoelastic response of the membrane. In addition, the time taken to recover the deformation of flexible membranes is another critical factor in the design of flexible membrane-based electromagnetic actuators.[116]

Magnetorheological (MR) fluid changes its apparent viscosity when exposed to a magnetic field. This phenomenon happens because the magnetic microparticle suspended in MR fluid aligns with the magnetic flux lines. Hence, MR fluid-based flexible actuators can be locally controlled by exposing a specific area to a magnetic field. McDonald et al.[113] developed a soft actuator integrating MR fluid valves, Fig. 3C. Here, the MR fluid circulates through the flexible actuator structure using an external pressure source. As a magnetic field is applied, magnetic particles in the MR fluid align with the magnetic flux lines and induce a local increase in viscosity. This phenomenon creates a valving action and causes a pressure increase between

the source and the location where the magnetic field is applied, consequently resulting in the deflection of the actuator structure. Electromagnets can be used to control the magnitude of the field, which in turn controls the viscosity of the magnetorheological fluid.

Magnetic nanoparticles suspended elastomeric soft actuators show promising performance for localised and distinctive deformation.[117] The stiffness of the flexible structures used for the soft actuators reduces under magnetic fields while increasing the maximum actuator force. Lee et al.[117] revealed that Fe_3O_4 suspended PDMS tubular structure showed a 3500% improvement in blocking force while reducing the stiffness of the elastomeric matrix by 85% when exposed to a magnetic field.

Magnetic hydrogels are thermosensitive polymers embedded with magnetic nanoparticles.[122] Embedding functional additives such as magnetic nanoparticles enable the non-contact operation of hydrogel-based soft actuators. Magnetic hydrogels undergo a magnetothermal effect where the magnetic nanoparticles dissipate heat to the thermosensitive polymer network. Heat dissipation happens based on two mechanisms. When the magnetic particles rotate while a fixed magnetic moment is applied along the crystalline axes (Brownian rotation), heat generation occurs due to the shear stress in the surrounding fluid. In contrast, if the magnetic particle remains stationary while the magnetic moment rotates (Néel rotation), the heat generation occurs due to the rearrangement of atomic dipole moments within the particle.[123] So, the magnetisation of magnetic hydrogels is low under a static magnetic field. The improved magnetisation of the magnetic hydrogels can be obtained under an alternating magnetic field (AMF) whose amplitude varies with time.[118] Also, adding more magnetic nanoparticles to the hydrogel would result in higher magnetisation, and a higher magnetothermal effect causes the thermosensitive polymer network to shrink. Tang et al.[118] developed elastomer-magnetic hydrogel bilayer elements to create shape-morphing structures under AMFs. Strong adhesion between magnetic hydrogel layers and the elastomer is crucial for the bending performance of the flexible structure, Fig. 3D.

Magnetic shape memory materials (MSMM) can be used to develop micropumps where the MSMM material serves simultaneously as valves, channels, and pumps.[119] A diametrically magnetised permanent magnet was rotated to create an identical magnetic field along the cross-section of the MSMM element, where the shrinkage of the material allowed the fluid to move from the inlet to the outlet, Fig. 3E. The shrinkage of the MSMM happens due to the magnetic field, and it will enable fluid to enter through the inlet. Then fluid moves along the channel because of the shrinkages created by the movement of the magnetic field. This method is capable of contact-free pumping of various liquids, including air, and is self-priming.[124] The MSMM micropump developed by Smith et al.[119] has a 6 μm thick Ni–Mn–Ga element that creates 30 μm shrinkage under the effect of a

Table 3 Magnetic actuation principles

Actuation	Actuator type	Dimensions	Material(s)	Fabrication method(s)	Magnetic field (T)	Mode of actuation	Deformation	Force	Application(s)	Ref.
Electromagnetic	Shape morphing surfaces	Ribbon: L – ~48 mm W – 900 μm T – 400 μm Membrane: T – 5 μm	Dragon Skin™, Ecoflex™, EGaIn	Laser cutting, soft lithography	~0.2	Out-of-plane reversible deformation	2.4–9.6 mm	0–4.8 mN per ribbon	Tunable optics, flexible/stretchable electronics, soft machines, biomimetic skins	111
	Micro pumps	Membrane: D – 5 mm T – 400 μm Magnet: D – 700 μm T – 1.4 mm	PDMS, stainless steel	PDMS casting, spin coating, thermal bonding, μWEDM	0.11	Reciprocating	8 μm	NA	Fluid handling	112
MR fluid-based	Soft structures	Structure: L – ~4 cm W – ~1.5 cm T – ~3.5 cm Magnet: D – 12.5 mm T – 12.5 mm	Dragon Skin™, Ecoflex™, acrylic sheets, silicone tubes, MR fluid	Laser cutting, spin coating	0.02	Out-of-plane flexion and extension	NA	NA	Medical robotics	113
Magnetic hydrogel-based	Shape morphing structures	L – 20 mm W – 2 mm T – 2.05–2.55 mm	Magnetic PNIPAm, very-high bond tapes	Laser cutting, adhesive bonding	0.15@187 kHz	Flexion and extension	0.23 mm^{-1}	NA	Robotics, biomedicine	118
MSMM	Micro pumps	Element: L – 10 mm W – 2.5 mm T – 1 mm Pump: L – 17.5 mm W – 10 mm T – 4.7 mm	Ni–Mn–Ga MSMM, polycarbonate, PDMS	Wire sawing, electropolishing, mechanical polishing, curing	0.5@135 Hz	MSMM twinning and recovery	NA	NA	Lab-on-a-chip, point-of-care diagnostics	114, 119

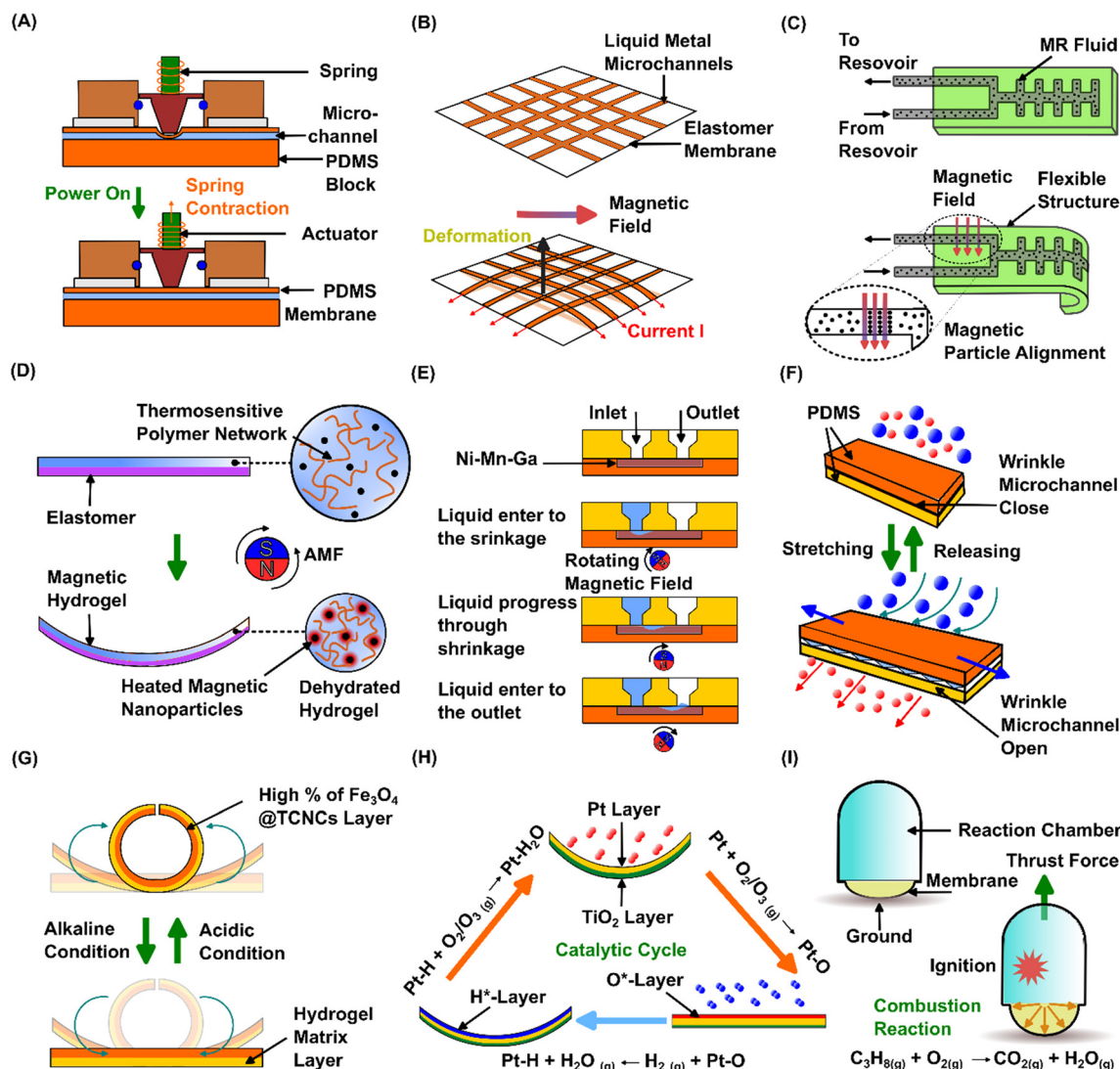L – length; W – width; T – thickness; D – diameter.

Fig. 3 Further actuation schemes. (A) Normally-closed electromagnetic (EM) microvalve opens by the electromagnetic actuator that works against the spring force.[116] (B) A Lorentz force-based shape morphing structure shows arbitrary shapes under selective current supply through liquid metal conductors.[111] (C) A magnetorheological (MR) fluid-based flexible actuator deforms under blockage of the fluid flow by magnetic particles that concentrated at the locally applied magnetic field.[113] (D) Shape morphing of hydrogel in an alternating magnetic field (AMF).[118] (E) Magnetic shape memory alloy micropump operates under rotating magnetic field.[119] (F) Strain-tuneable wrinkle microvalve for selective transfer of particles by stretching.[47] (G) Asymmetric hydrogel actuators deflect under variation of pH around the actuator structure.[120] (H) Surface-catalysed chemical actuator operates under moisture absorption and undergoes catalytic reaction.[46] (I) Chemical combustion-driven soft actuator.[121]

500 mT magnetic field. The micropump could deliver a water volume of 110 ± 15 nL per pumping cycle. The pumping characteristics depend on the surface effects and viscosity of liquids.

2.4. Mechanical strain-based actuation

Mechanical strain-based actuation utilises mechanical forces to bend,[125] twist,[126] and stretch[47] microdevices to achieve specific functions. Actuation is entirely based on stretching[47] or combining electric fields,[127–130] magnetic fields,[131] and temperature sources[132,133] to generate displacements and forces. However, mechanical deformation in initiating and supporting actuation cycles is significant in this actuation

method. Table 4 summarises and compares parameters related to the design, fabrication and performance of some reported mechanical strain-based actuators.

Actuators based on mechanical strain consist of structures such as layers,[47] flat wires,[80] capsules,[133] membranes,[134] and thin films.[132,135] This actuation scheme is a promising strategy in microfluidics to control fluid flow, serving as microvalves,[47,80] and micropumps.[133] For example, Kotb *et al.*[133] developed a micropump that integrates all components in a self-contained package to reduce the overall footprint, defined as a capsule micropump. The actuation happens by the temperature-induced strain of the shape memory alloy (SMA), and the recovery motion occurs through the elastic forces of the capsule material acting as a spring.

Table 4 Mechanical strain–based actuation principles

Actuation	Actuator type	Dimensions	Material(s)	Fabrication method(s)	Stress/strain	Mode of actuation	Deformation/speed	Force	Application(s)	Ref.
Mechanical stretch	Crack and wrinkle microvalves	L – 3 cm, W – 1.2 cm, T – 1.2 mm	PDMS	Stretch-assisted micro irregularity formation, UV exposure	0–75%	Stretching and releasing	Crack: ΔW = 18 μm, ΔH = −2 μm	NA	Cell-sorting, fluidic logic gates, biomedicine	47
Buckling-guided electro-mechanical	Dielectric elastomer (DE) actuator	L – 180 μm to 6 mm, T – 8 μm to 50 μm	Celular graphene, PI, PET, Au, very-high bond tapes	Spin coating and curing, femtosecond laser cutting, metal deposition	Intermediate pre-strain: 150% to 230%, Nominal strain: ~80%	Out-of-plane	Ribbon mesostructure: ~6 mm	NA	Morphable 3D capacitors for LC-radio frequency circuits	127
	Piezoelectric (PZT) actuator	PZT: L – 200 mm, W – 140 mm, T – 500 nm	SU-8, PZT, Ti/Pt, Cr/Au, PI, Dragon Skin™	Sol-gel techniques, photolithography, and etching, electron beam evaporation, transfer printing	Maximum strain: PZT: 0.3%, Electrode: 1.2%, SU-8: 3.5%	Out-of-plane	NA	NA	Mechanobiology, energy harvesting	128
Smart material	Micropumps	NiTi wire: D – 0.25 to 0.5 mm, Pump: V – 424.7 μL	NiTi wires, Ecoflex™	Moulding, coiling, 3D printing	NA	Linear	5.6 mm, 11 mm s^{-1}	NA	Drug delivery	133

L – length; W – width; T – thickness; D – diameter; H – height; V – volume.

The micropump can produce large strokes as the actuation follows the direction of the highest mechanical compliance with almost zero dead volume. Apart from the above concepts, mechanical instabilities or micro-patterns such as microcracks and micro wrinkles have been utilised as microvalves,[47] Fig. 3F. These microvalves open and close by stretching and releasing. Liu *et al.*[47] demonstrated that the size of the triangular microcracks shrank from 2.8 μm in width and 5.8 μm in height to 20.8 μm and 3.8 μm, respectively, when a 75% tensile strain was applied. As the applied strain exceeds 100%, the microvalves tend to break. The flow rate through the crack microvalve monotonically increased from 0.04 mm^3 s^{-1} to 0.34 mm^3 s^{-1} as the tensile strain rose from 25% to 100%.

Mechanical strain-based schemes can also create three-dimensional (3D) actuation.[127,128] 3D actuation is achieved by a pre-stretched elastomer substrate. In these designs, the 2D precursor structures are coated on a pre-stretched elastomer substrate.[127,128] Releasing the pre-stretched condition enables coordinated bucking-guided transformation, resulting in 3D structures. After forming the 3D structures, active materials such as lead zirconate titanate (PZT),[128] SMA[80,133] or elastomer materials with inherent dielectric properties[127,136] could actuate these highly flexible structures. The out-of-plane actuation performance and output force of strain-based schemes can be improved by introducing hybrid materials with enhanced dielectric and mechanical properties.[137]

In addition, multilayer stacked structures[138] can improve the force output to achieve bi-directional actuation. Dielectric elastomer (DE) and PZT materials are promising candidates for strain-based actuators. In DE materials, coordinated deformations, such as translation, rotation, bending, and twisting, depend on the selected bonding locations of DE and strain-limiting fibres in the dielectric substrate. Strain-limiting fibres can constrain the displacements along desired linear or radial directions.[127] The overall performance of the DE actuators (DEAs) depends on the stiffness of the material, the dielectric constant, and the breakdown voltage. In contrast, PZT materials bonded with elastomeric substrates cannot achieve the large deformation of DEAs, but generate higher mechanical forces.[128] Meanwhile, shape memory alloy (SMA) actuators can provide out-of-plane forces,[80] but their response speed is generally slower than others. Also, the resonant frequency of the SMA actuators influences the actuation speed and deformations. Song *et al.*[126] studied a bending actuator by changing the design of the reinforcement structure embedded in the actuator. The reinforcement structures are made of 38-μm diameter SMA wires embedded along the length of the actuator above and below an acrylonitrile butadiene styrene reinforcement structure consisting of 250 μm thick layers in different patterns located at the centre. The team found that the reinforcement structure led to a change in the natural and actuation frequencies of the actuator.

2.5. Chemical actuation

Chemical actuation refers to the use of materials that can undergo controlled strokes and forces in response to chemical stimulations, such as pH change,[120] surface catalysis,[46] moisture gradient,[139,140] organic solvent stimulations,[141] oscillatory Belousov–Zhabotinsky chemical reaction in hydrogel,[142] and chemical combustion.[143] Chemical stimulation through pH change can actuate materials that exhibit reversible deformations under alkaline and acidic solutions,[120] Fig. 3G. Surface-catalysed chemical actuators utilise catalyst-treated surfaces to speed up the reactions and generate surface stresses,[46] Fig. 3H. Moreover, moisture gradients[45,144,145] can achieve reversible actuation depending on the relative humidity of the environment. The deflection follows the absorption and desorption of water molecules, enabling moisture-driven microactuation. In addition, organic solvents in the form of liquids and vapor[141] can be used to stimulate materials that undergo swelling on the absorption and recover on desorption of the solvent molecules. The self-oscillatory Belousov–Zhabotinsky chemical reaction of synthetic polymer gels can convert chemical energy to useful mechanical work. This chemical reaction causes a large volume change. Aishan *et al.*[142] developed a micropump based on this actuating scheme where a PDMS membrane deflects by the large volume change of the polymer gel during the oscillatory Belousov–Zhabotinsky reaction. This pump generates a 0.28 μL min^{-1} net flow rate. Chemical combustion-based actuation uses combustion reactions to generate energy that can be effectively used in actuation tasks,[146,147] Fig. 3I. However, quantifying actuator deformations and forces remains a challenge due to the complex and dynamic nature of the combustion process.[148] Yang *et al.*[121] developed a combustion actuator operated through the combustion of a propane and oxygen mixture. The actuator consists of a combustion chamber and a membrane. The team developed a theoretical model to investigate the effect of combustion reaction on membrane deformation and the magnitude of the thrust force.

Chemically driven microactuators mainly consist of multiple material layers[45,46,141] where one layer is susceptible to chemical variations and undergoes deformation, while the other layers serve as the biasing substrate to support reversible actuation strokes. However, the multilayer approach is unstable in the long-term operation due to interfacial instabilities. Therefore, asymmetries within the same material were used to avoid this issue.[120] Furthermore, the recent development of advanced synthesised materials[144,145] is an emerging trend in chemical actuation to replace the multilayer approach. The state-of-the-art surface-catalysed chemical actuators developed by Bao *et al.*[46] demonstrated a complete actuation cycle within 600 ms at an average actuation rate of 0.8 μm^{-1} s^{-1}. In contrast, hydrogel actuators have limited capability for actuation speed but can be used for slow actuation. The frequency of hydrogel-based chemical actuators depends on deswelling rates in mediums of different pH values.[120] The directional deformations of Polypyrrole-based actuators can be programmed by predefined

cutting lines of the material layers[45] because the deformations under moisture variations happen along the cutting lines. Ge *et al.*[144] developed cellulose nanocrystal-derived photonic materials with promising flexible sensing and actuating characteristics. The actuator showed high bending angles (135° to −136°) and bending rates (4.6° s^{-1}). The moisture-driven actuators based on Ti$_3$C$_2$T$_X$ MXene graphene film exhibited larger bending angles, faster-bending speeds up to 32° s^{-1}, reversible deformations, and good stability in actuation cycling.[145] The MXene graphene oxide films could lift loads many times heavier than their weight. Wang *et al.*[141] reported an organic solvent stimulus actuator consisting of carbon nanotubes (CNTs) padded in a PDMS layer connected with a poly (vinylidene fluoride) (PVDF) layer by a PDMS connection layer (PDMS/CNTs–PDMS–PVDF). This sandwich layer arrangement can undergo large deformations at shorter response time. The structure can swell due to the absorption of *n*-hexane molecules and bend towards the PDMS/CNTs layer in 10 ms, exhibiting a fast response. The bending angle can reach up to 900° depending on the stimulation location, and the bending angle can be accurately adjusted by changing the solvent type. Table 5 summarises and compares parameters related to the design, fabrication and performance of some reported chemical actuators.

3. Materials for actuators and flexible microdevices

Materials for flexible and stretchable devices should comply with the actuation principles. Very often, the actuators and the flexible microdevices are fully integrated into one platform and made of the same materials. It is challenging to differentiate explicitly between the actuators and the flexible devices being actuated. Therefore, we will discuss the fabrication materials and methods for flexible devices and actuators. A wide range of polymeric materials, electrically conducting materials, silicon, and glass have been used to construct flexible devices and actuators. Fig. 4 compares the characteristics such as elastic modulus and maximum strain of common materials used in flexible and stretchable microdevices.

3.1. Polymeric materials

Polymeric materials such as thermoplastics, elastomers, and thermoplastic elastomers[34] are widely used in actuators and flexible devices. Table 6 compares Young's modulus, tensile strength, and maximum strain for these materials and summarises their advantages, limitations, and applications.

Polydimethylsiloxane (PDMS) is an elastomeric polymer containing carbon and silicon. PDMS has advantages such as durability, corrosion resistance, biocompatibility, and high optical transparency.[22] In addition, the low shear and Young's modulus, high strains at fracture, and ease of manufacturability enable the utilisation of PDMS in pneumatic[52,57,58,63,64] and hydraulic microactuators.[55] Microdevices such as micropumps and microvalves are

Table 5 Chemical actuation principles

Actuation	Actuator type	Dimensions	Material(s)	Fabrication method(s)	Stress/strain	Mode of actuation	Deformation/speed	Force	Application(s)	Ref.
pH change	Asymmetric hydrogel actuator	L – 28 mm, W – 2 mm, T – 1 mm	Fe_3O_4@TCNCs, acrylic acid, acrylamide	In situ polymerisation, magnetic field-assisted patterning	Tensile strength: 228 kPa, Maximum strain: 872%	Out-of-plane	Angular – 601°, 30° min^{-1}	NA	Artificial muscles, photonic displays, soft manipulators	120
Moisture gradient	Supercontractile polymer actuator	Tensile test specimen: L – 15 mm, W – 5 mm, T – 90 µm	Poly(ethylene oxide), poly(ethylene glycol)-α-cyclodextrin inclusion complex	Cold drawing	400%	Contraction and expansion	Contraction: ~60% within 2 s	~0.13 N, 60% decaying in 10 s	Biomedical	140
	Janus actuator	L – 20 mm, W – 3 mm	Cellulose nanopaper, reduced graphene oxide, lignin, graphene oxide	Vacuum filtration, reduction, drying	Tensile strength: 141 MPa, Maximum strain: 5%	Out-of-plane	~9.6° s^{-1} @ RH-70%	NA	Bionic devices, humidity sensors	139
Organic solvent stimulation	Strip-shaped actuator	L – 8.5 mm, W – 2 mm, T – 181 µm	PDMS/CNTs, PVDF, PDMS	Electrospinning, bonding	NA	2D rotary-spiral	Angular – 900° @ 15.76 s	NA	Healthcare, bioengineering, soft robots	141
Chemical reactions	Surface-catalysed chemical actuator	SiO_2 panels: L – 20 µm, W – 30 µm; T – 0.5 µm; TiO_2 layer: T – 2 nm; Pt film: T – 7.5 nm	Pt sheets, TiO_2, SiO_2, Al and Al_2O_3	Standard semiconductor process	NA	Out-of-plane	Translational: 10 µm, Angular: 45° @ 2 v% H_2, 0.8 $µm^{-1}$ s^{-1}	NA	Robotics, medical devices	46
	Micropumps	Membrane: D – 5 mm, T – 100 µm	Synthetic polymer gel, PDMS, glass	PDMS replica moulding and plasma bonding, polymer moulding	NA	Reciprocating	109.77 ± 12.39 µm	0.07 mN	Wearable devices, lab-on-a-chip	142
	Combustion actuator	Membrane: D – 60 mm, T – 8 mm; Chamber: H – 125 mm, D – 100 mm, V – 80 cm^3	Dragon Skin™	Centrifuging, vacuum defoaming and curing	NA	Out-of-plane	70 mm @ premixed ratio: 3 with 30 mL reactants	630 N	Soft robotics	149

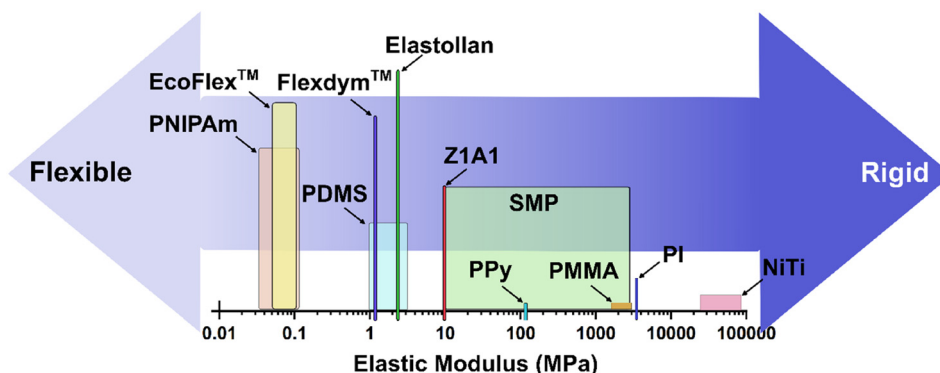L – length; W – width; T – thickness; D – diameter; H – height; V – volume.

Fig. 4 Characteristics of the materials used for flexible and stretchable actuators. The height of the columns represents the maximum obtainable strains (see Table 6) for the respective materials.

generally made of multiple stacked layers, such as the supporting, fluidic, and control layers. PDMS is commonly utilised for the fluidic layers with flexible membranes due to its superb elastic properties. However, PDMS also has several limitations, such as its hydrophobic nature, porosity, and solvent incompatibility. The methyl (CH_3) groups in PDMS make the surfaces hydrophobic (contact angle with water $\sim108^0$)[22] limiting the applications such as electrophoretic separation[150] and droplet formation[151] in microfluidics that require certain wettability of microchannel surfaces. However, methods such as Oxygen plasma treatment[152] and surface coatings[153] can be used to make the PDMS surfaces hydrophilic. Moreover, PDMS materials have a certain porosity depending on curing conditions that can affect functionality in applications. These pores increase the surface area making absorption of small molecules altering the outcomes of quantitative analyses.[154] However, in terms of mechanical performance of flexible and stretchable microdevices, porous PDMS provides enhanced flexibility than non-porous PDMS. Certain solvents[155] cause the PDMS to swell leading to changes in microchannel features.

PDMS has been used in multi-material electro-thermal actuators. In these applications, non-metallic bi-morph actuation[72,88] was implemented by combining materials such as polyimide (PI) and graphene with PDMS to form PI–PDMS,[72,77,88] and Graphene–PDMS[84] bilayer structures. In addition, acrylic-based photoresist materials, such as IP–PDMS (Nanoscribe GmbH)[25] and IP–S (Nanoscribe GmbH),[85] have also served as bi-morph structures. Their coefficient of thermal expansion (CTE) can be tuned by adjusting the degree of polymerisation. As an elastomer, PDMS is a suitable material for thermo-pneumatic actuators.[81] The elasticity of PDMS structures can be tuned by altering the composition of the pre-polymer and curing agent[156] as well as the curing temperature[157] to obtain the required flexibility.

PDMS has been used as the flexible membrane for microvalves and micropumps with electromagnetic actuation.[112,116] PDMS has a constant monotonic elastic modulus regardless of the influence of thickness and tensile loading.[158] The PDMS reaches a steady state rapidly upon

deformation,[159] allowing better performance with high-frequency electromagnetic actuation. Iron oxide (Fe_3O_4) nanopowder can be mixed with PDMS to form a magnetically responsive flexible material.[117] Carbon black particles were embedded in PDMS to form PDMS-encapsulated carbon black (PCB) and mixed with vinylsilane-rich silicone (VRS) to create PCB/VRS hybrid layers. The enhanced conductivity reduces the high operating voltages for silicone-based dielectric elastomer actuators, minimising the electrical breakdown and the creep rupture.[137] PDMS was also used to fabricate microcracks and microwrinkles-based microvalves[47] due to the unique properties of the material, such as high elasticity, flexibility, and compatibility with the manufacturing process.

Ecoflex™ is a commercial silicone elastomer that has recently become popular in highly flexible and stretchable devices.[160] The material has several advantages, such as low Young's modulus, high flexibility, tear strength, and large elongations. However, the material has limitations such as high viscosity and low chemical resistance. Ecoflex™ has gained attention in the development of flexible microfluidic devices, biomedical applications, and soft robotics. For instance, the material was used to fabricate microchannels for magnetorheological fluid-based flexible actuators.[113] Dragon Skin™ is another commercial silicone elastomer material that is used for highly stretchable yet strong skin-like layers.[161] This material has a higher Young's modulus and tensile strength than Ecoflex™ and has been used as the strain-limiting layer of flexible actuators.[113] Dragon Skin™ material is also used to develop soft actuators with different layer stiffnesses for soft robotic grippers.[162]

Thermoplastic elastomer (TPE) is a rubber-like material that combines the properties of thermoplastics and elastomers. Flexdym™ is a commercially available TPE material used in microfluidics[20,163] because of its advantages such as high optical transparency, lower sweat absorption and water vapour transmission rate, and biocompatibility. Wu et al.[20] developed a skin-interfaced flexible microfluidic device for sweat capture analysis. However, it is expensive at the prototyping stages, and the bonding treatments involve harsh conditions such as volatile chemicals and high-temperature.

Table 6 Polymeric materials for flexible and stretchable microdevices

Material	Young's Modulus (MPa)	UTS (MPa)	Maximum strain (%)	Advantages	Limitations	Potential applications	Ref.
Polydimethylsiloxane (PDMS)	1–3	3–5	100–300	Low shear and Young's modulus, high optical transparency, durability, corrosion resistance, biocompatibility	Hydrophobic nature, incompatibility with solvents	Biomedical devices	34, 156, 157, 175, 176
Silicone elastomers (SE) (e.g., Ecoflex™)	0.05–0.1	0.37–1.7	500–800	Low Young's modulus, high flexibility, high tear strength, and large elongation	Opaque, high viscosity, low chemical resistance	Prosthetic appliances	34, 156, 176, 177
Thermoplastic elastomers (TPE) (e.g., Flexdym™)	1.18	7.6	720	High optical transparency, lower sweat absorption and water vapour transmission rate, biocompatible	Expensive to use at prototyping stages, requirement of bonding treatments with harsh chemical and temperature conditions	Microfluidic diagnostic applications	20, 163, 178, 179
Thermoplastic polyurethane (TPU) (e.g., Elastollan, Z1A1)	2.4, 9.2	2, 27.7	893, ~400	High flexibility and elasticity, chemical resistance, ease of 3D printing	Hygroscopic nature	Wearable devices	20, 176, 180
Polyimide (PI)	3450	231	72	Biocompatibility, high thermal stability, good sealing properties, chemical inertness	Opaque, hygroscopicity	Medical devices	34, 181, 182
Polymethylmethacrylate (PMMA)	1800–3100	48–76	5	High optical transparency, Low water absorption, biocompatibility	Low chemical resistance, susceptibility to warpage and porosity, poor fatigue resistance	Instrument displays	183, 184
Poly(N-isopropyl acrylamide) (PNIPAm)	0.035–0.105	0.35–0.65	600	Structural tunability, low toxicity, temperature-responsive reversible sol-to-gel phase transition	Low biodegradability, low drug loading capacity, poor mechanical strength	Thermo-responsive biomedical applications	165, 167, 185, 186
Shape memory materials (SMM) (e.g., shape memory polymer (SMP), NiTi)	SMP: 10–3000, NiTi: M: 28000–41000, A: 75000–83000	895	SMP: >400, NiTi: <10	SME and PE, corrosion resistance, biocompatibility, high energy density per unit volume of material	High fabrication cost	Flexible medical devices	23, 105, 187, 188
Polypyrrole (PPy)	108.57	61	4	Biocompatibility, ease of synthesising, low cost	Water insolubility, instability	Tissue engineering	45, 189, 190
Cellulose nanocrystals assembled poly(ethylene glycol) dimethacrylate [CNC-poly(PEGDMA)]	~3	42	104	Improved solvent resistance, impressive toughness, and strength, vivid optical iridescence under strains	Requirement of sophisticated and careful fabrication methods	Drug delivery, intelligent actuators	144, 191

A – austenite, M – martensite.

Thermoplastic polyurethane (TPU) is an elastomeric material that exhibits the properties of plastics while showing the flexibility of rubber material. Its high flexibility and chemical resistance allow for a variety of applications. Shaegh *et al.*[54] used TPU as the flexible element in pneumatic micropumps. TPU has gained attention because of its compatibility with fused deposition modelling (FDM) 3D printing technology.[164] FDM creates 3D components by extruding thermoplastic filament in a series of layers. Properties such as flexibility, conformability, and excellent interlayer adhesion make TPU a better candidate for FDM technology. However, the hygroscopic nature of the material is the limiting factor in applications.

Polymethylmethacrylate (PMMA) is a synthetic polymer commercially known as Perspex or acrylic glass. The advantages of PMMA are high optical transparency, low water absorption, and biocompatibility. PMMA has been used to fabricate the supporting layers in micropumps and microvalves.[53,54] The drawbacks of PMMA include poor fatigue resistance, susceptibility to warpage, and low chemical resistance.

Hydrogels consist of a hydrophilic polymer network that can swell under the absorption of moisture and also hydrogels are thermo-responsive. Temperature increase collapses the polymer networks, leading to high volume shrinkages. Hydrogel materials such as poly(*N*-isopropyl acrylamide) (PNIPAm) possess a lower critical solution temperature of around 32 °C,[165] where the material changes from hydrophilic to hydrophobic nature. In addition, PNIPAm enables the development of flexible actuation structures with autonomic perspiration capabilities. Autonomic perspiration is sweating due to increased temperature through the dilation of a pore structure located on the actuator body. This process is essential to thermoregulate actuators operating at peak power for an extended period.[166] This material is promising for biomedical applications due to excellent structural tunability and low toxicity. The covalent bond of the polymeric chains in hydrogel promotes the easy construction of multilayer structures in actuators.[69,70] However, the elastic modulus of the hydrogel is low compared to polyurethanes and silicones. Thus, adding a small amount of hydrophilic polymer networks such as alginate can enhance the mechanical toughness of hydrogel.[69,70] Furthermore, synthesised hydrogel materials with co-precipitating Fe_3O_4 nanoparticles of tunicate cellulose nanocrystals (TCNCs) (Fe_3O_4@TCNCs) form asymmetric hydrogel materials.[120] TCNCs enable better mechanical properties of hydrogels. Similarly, hydrogel responsive to magnetic fields can be prepared by precipitating Fe_3O_4 magnetic nanoparticles in the PNIPAm nanocomposite hydrogel matrix.[118] Despite many advantages, hydrogel materials have low biodegradability and limited mechanical strength.[167]

Polymeric materials such as polypyrrole (PPy) with particular patterns can be combined with inert polyethylene terephthalate layers to form humidity-sensitive bilayers.[45] Here, the PPy is electrochemically synthesised and doped with perchlorate to rapidly expand the material on water vapour absorption. PPy is suitable for developing microactuators because of its biocompatibility and simple synthesis. Moreover, cellulose nanocrystals (CNCs) assembled poly(ethylene glycol)dimethacrylate (PEGDMA) monomers in *N*,*N*-dimethylformamide can be synthesised to form flexible and stretchable materials sensitive to humidity variation. Ge *et al.*[144] reported a CNC–poly(PEGDMA) made of equal amounts of CNC and PEGDMA with 104% in stretchability, 42 MPa in mechanical strength, and 31 MJ m^{-3} in toughness.

Resins, such as IP–DIP (Nanoscribe GmbH),[68] have also been used to develop highly flexible actuator structures for microhydraulic actuators. Smith *et al.*[68] have used IP–DIP (Nanoscribe GmbH) resins to develop hydraulically actuated flexible bellows structures with a sidewall thickness of 1 μm.

Dielectric elastomers belong to the group of electroactive polymers. Dielectric elastomers produce large strains as an electric field is applied to the material. High-performance dielectric elastomers should have low stiffness, high dielectric constant, and high electrical breakdown strength. Dielectric elastomers are most popular in mechanical strain-based flexible and stretchable actuators[168] due to their advantages of high energy density, fast response, and large obtainable strains.[169] Polyvinyl chloride (PVC)-based dielectric elastomers demonstrate high actuation performance under low actuation voltages.[43] Moreover, pentablock copolymeric elastomers such as $(SEHAS)_2$ can form high-performing soft microactuators, which work under relatively low voltages in contrast to the common driving voltage on the order of kilovolt. Chen *et al.*[135] reported a $(SEHAS)_2$-based ultra-thin actuator that operates under 680 V, providing a 93% strain. Piezoelectric polymers also belong to the electroactive polymers which produce mechanical deformation in response to an applied electric field. Poly(vinylidene fluoride) (PVDF) is one of the promising piezoelectric polymers due to its high efficiency and mechanical stability as well as fast response.[170] The conversion efficiency from electrical to mechanical energy is highly affected by the polarisation of the molecular structure.[171] Won *et al.*[172] reported an ultrafast, and programmable molecular structure transition process that uses continuous wave laser together with gold nanoparticles that enhance the thermal effects induced by the laser. They integrated monolithic PVDF layers to achieve a frequency-driven soft robot.

3.2. Electrically conducting materials

Apart from polymeric materials, electrically conducting materials have been used in flexible and stretchable actuators. Examples of electrically conducting materials for actuators include metals such as shape memory alloys (SMAs), stainless steel, aluminium, metal–silicone composites, Pt, TiO_2, MXene, and derivatives of graphene such as graphene oxide (GO).

SMAs are a class of shape memory materials (SMMs)[105] sensitive to temperature variations and undergo solid phase transformation, showing large recoverable strain that plays a significant role in strain-based actuation.[75] SMMs possess unique characteristics of the shape memory effect,[173] which is substantial in electrothermal actuators and pseudoelasticity.[80] In addition, magnetic shape memory materials show crystallographic changes and deform upon applied magnetic fields. Magnetic shape memory materials such as Ni–Mn–Ga were used to develop magnetically operated micropumps.[119] SMA-based microactuators provide the most promising energy density compared to other actuation concepts,[80] despite their slow actuation frequency because of the requirement of efficient cooling.

Materials are combined to develop multi-material electro-thermal actuators. For instance, bi-morph actuation could be implemented using metals such as aluminium–nitinol.[83,87] However, the non-metallic bi-morph actuators require a separate heating circuitry to increase the temperature in non-metallic layers. These conductive paths were made of liquid metals such as eutectic GaIn[72] and Galistan.[85] Also, the conductive paths for electrothermal actuators can be directly formed on polymeric materials. The conductive layers, such as laser-induced graphene,[77,88,174] were formed with good electrical conductivity. Moreover, graphene was used as a layer to form bi-morph structures, eliminating the additional electrical circuitries.[84]

In addition, EGaIn in silicone elastomer has been used in electromagnetic membrane actuators.[111] Stainless steel was used for mass-spring structures in electromagnetic actuators to support flexible membranes.[112] Aluminium is a suitable material for bent-beam actuators that require robustness and reliability.[79] Metal–silicone composites have also been used to make bent-beam actuators where the introduction of metal layers significantly reduces electrical resistance, resulting in low driving voltages.[101]

Materials such as Pt and TiO_2 have been used for bimorph actuation elements in surface-catalysed chemical actuators. The PtO_x layers on the Pt material react with H_2 and O_2/O_3, and the induced surface stresses cause the bending of the structure.[46] Besides, $Ti_3C_2T_X$ MXene and graphene oxide (GO) materials can be combined to form MXene graphene oxide (MGO) film actuators that are fast, reversible, and have good cycling stability.[145] The introduction of GO can significantly lessen the inherent brittle nature and rapid oxidisation of MXene.

3.3. Other materials

Glass,[51,59–61] and silicon[56] have been used in the supporting layers of the microdevices, such as micropumps and microvalves. Silicon was also used as a flexible element in pneumatic microvalves.[56] In addition, silicon was employed in pseudo-bi-morph and bent-beam microactuators based on the silicon-on-insulator substrate.[96] Silicon-on-insulator actuators have been widely employed[101] due to their excellent compatibility with materials for microelectronics and microelectromechanical systems.

4. Fabrication methods for actuators and flexible microdevices

4.1. Photolithography and soft lithography

Photolithography and soft lithography have been extensively used to fabricate flexible microdevices,[51,56] Fig. 5A. In photolithography, masks pattern photosensitive materials coated on a substrate after exposure to ultraviolet (UV) light, Fig. 5A(i). The exposed or unexposed photosensitive photoresist is selectively removed by a developer to obtain the required patterns depending on its properties. The exposed region is removed when using a positive photoresist, and the unexposed region is removed when using a negative photoresist.[192] Photolithography can then be combined with other methods, such as etching and deposition, to form microstructures for microdevices. Shibamoto et al.[56] used photolithography and deep reactive ion etching to fabricate pneumatic microvalves. In addition, hot and cold arm microactuators were manufactured by integrated circuit fabrication technology, mainly involving sputtering and etching processes, where the subsequent fabrication steps were assisted by photolithography.[96] Foundry services such as multi-user MEMS process (MUMPs®) utilising silicon-on-insulator structures, also known as SOIMUMPs™,[26] use photolithography as a subsequent step. SOIMUMPs™ was used to fabricate bent-beam actuators.[42,103] Moreover, SOIMUMPs™ allows for making multiple devices on a single silicon wafer. Thermal expansion-based actuators and phase change actuators, such as SMA-based thin film microactuators, can be fabricated by micromachining processes such as low-pressure chemical vapour deposition, sputtering, wet etching, and reactive ion etching that involve photolithography in these subsequent steps.[132,193]

Soft lithography transfers the inverted patterns from a mould or master to elastomeric materials, Fig. 5A(ii). In this technique, the individual layers are made by pouring elastomer materials such as PDMS onto the SU-8 moulds. The solidified layers are peeled off and bonded after surface preparation under ultraviolet light irradiation in a vacuum. Soft lithography is frequently used to fabricate microdevices such as pneumatic micropumps[51,59–62] and microvalves.[52,57,63,64] This fabrication technique has also been used for hydraulically actuated microdevices.[55] Ni et al.[111] reported an electromagnetic actuator with liquid metal embedded in the microfluidic structures. The microchannels were formed in the thin PDMS layers using soft lithography and laser cutting[111,113] and bonded to a thin silicone membrane.

4.2. Additive manufacturing

Additive manufacturing is a technique to manufacture three-dimensional objects by adding materials layer-by-layer,[194,195] Fig. 5B. Additive manufacturing is mostly famous and known as three-dimensional (3D) printing or fused deposition modelling (FDM) technology, Fig. 5B(i). Instead of the conventional material removal process to fabricate objects,
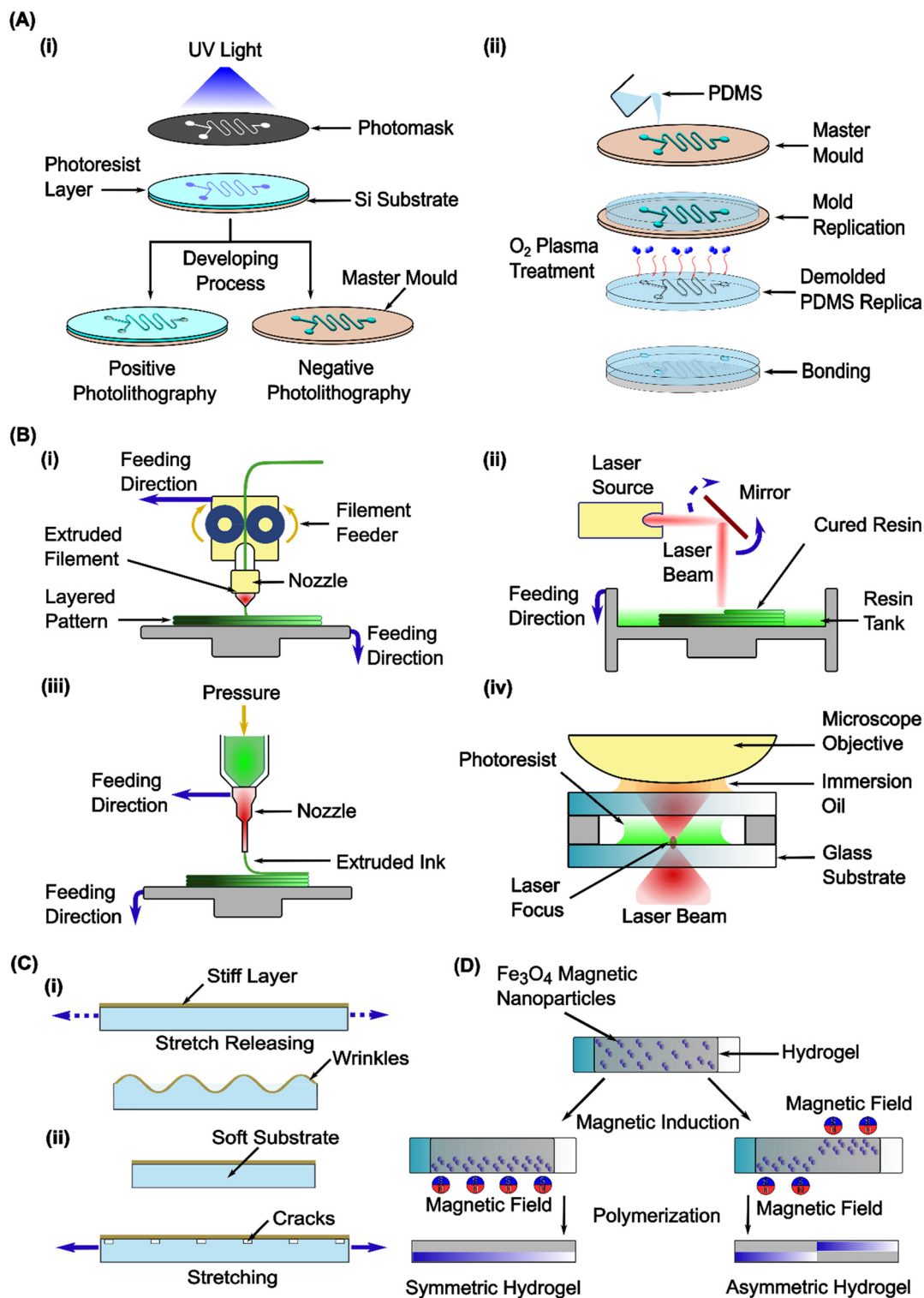
Fig. 5 Fabrication technologies. (A) Micropatterning. (i) Positive and negative photolithography, and (ii) soft lithography. (B) additive manufacturing technologies. (i) Fused deposition modelling (FDM), (ii) stereolithography (SLA), (iii) direct-ink-writing (DIW), (iv) two-photon polymerisation (2PP). (C) Crack and wrinkle microvalves formation through (i) prestretch releasing (wrinkle microvalves), (ii) stretching (crack microvalves). (D) Magnetic field assisted fabrication of asymmetric hydrogel structures.

additive manufacturing uses a layer-by-layer approach to generate 3D objects by depositing material layers according to a computer-generated model. 3D printing has the advantages of flexibility, short manufacturing time, and reduced material wastage. However, its resolution is generally lower compared to photolithography.

Additive manufacturing can eliminate the bonding process of multiple layers of soft lithography in fabricating flexible and stretchable devices. Microchannels fabricated by the soft lithography need to be sealed with another layer. In contrast, 3D printing can produce complex microchannel structures as a sacrificial mould that can be dissolved and removed. This technique is known as the embedded scaffold removing open technology (ESCARGOT).[27] This technique has been used to fabricate pneumatic microactuators to control fluid flow in a miniature fluidic system.[58] Moreover, 3D printing techniques can fabricate flexible and stretchable structures using soft polymeric and metallic materials. For instance, 3D printing was used to make conductive paths for non-metallic bi-morph actuator structures using EGaIn.[72] Polylactic acid (PLA)–carbon black-shaped memory polymer material and acrylonitrile butadiene styrene (ABS) were used to print conductive and non-conductive areas of a bent-beam actuator.[196]

Multi-material stereolithography (SLA) is one of the 3D printing techniques for fabricating multi-material structures, Fig. 5B(ii). This technique is a light-based approach that uses controlled photoirradiation to cure a liquid photopolymer ink selectively. SLA permits both micrometre resolution and rapid deposition rates. Recently, this method was used to fabricate a fluidic actuator using hydrogel.[166] In addition, direct-ink-writing (DIW) 3D printing permits complex structures of the modified hydrogel, including hollow and suspended features,[69] Fig. 5B(iii).

Two-photon polymerisation (2PP) is an advanced 3D printing technique based on two-photon absorption to polymerise a photosensitive material selectively, Fig. 5B(iv). This technique is superior in its high resolution and precision. Nano/micro scale 3D printing with 2PP[25] can be used to develop complex, compliant structures for flexible hydraulic actuators.[68] Moreover, 2PP four-dimensional (4D) printing[197] generates non-metallic bi-morph structures using the same material but making regions with different CTEs.[85] This method fabricated bi-morph microactuators capable of high rotational motions that are impossible to fabricate using the MEMS fabrication methods. However, 4D printing introduces the dimension of time to printed 3D structures as they evolve as a function of time.[198] This is done by the use of stimulus-responsive materials that enable functional adaptations.[199]

4.3. Other fabrication methods

Additionally to the fabrication techniques mentioned above, other fabrication techniques have also been developed for flexible and stretchable actuators, including microwire electro-discharge machining, ultrasonication, reversible/fragmental transfer emulsion polymerisation, pre-stretching, magnetic field-assisted *in situ* polymerisation, laser cutting technique, and ultraviolet light-triggered free radical polymerisation.

Some electromagnetic actuators utilise mass-spring structures that can be easily fabricated by the microwire electro-discharge machining.[112] Magnetic nanoparticle-suspended elastomeric materials can be synthesised through ultrasonication, giving rapid and uniform nanoparticle dispersion compared with high-speed shear mixing.[117] These elastomers are then spin-coated to fabricate the flexible magnetic responsive actuators through a layer-by-layer approach. In addition, magnetic bilayer hydrogel-elastomer actuators are prepared using adhesive bonding between very high-bond tapes and magnetic hydrogel sheets.[118]

Also, block copolymer structures of dielectric elastomer materials can be made by reversible/fragmental transfer emulsion polymerisation method, which improves the electromechanical performance of dielectric elastomer materials in the electric field-assisted mechanical strain-based actuators.[135] In addition, mechanical instability-based microdevices, such as cracks and wrinkle microvalves, are fabricated based on pre-stretching. In this method, releasing a pre-strained elastomer such as PDMS with a stiff surface layer results in wrinkled microchannels, Fig. 5C(i), and stretching the elastomer with a stiff surface layer leads to cracked microchannels,[47] Fig. 5C(ii).

Laser cutting can also create controlled patterns on polypyrrole polymer membranes, which are transferred to polyethylene terephthalate tape to create moisture-sensitive bilayer structures.[45] Ultraviolet light-triggered free radical polymerisation can be used to synthesise chiral nematic composites using cellulose nanocrystals and poly(ethylene glycol) dimethacrylate in *N,N*-dimethylformamide for humidity-sensitive actuation.[144]

Furthermore, asymmetric hydrogel materials can be fabricated by magnetic field-assisted methods, Fig. 5D. In that process, co-precipitated Fe_3O_4 nanoparticles on tunicate cellulose nanocrystals (TCNCs) (Fe_3O_4@TCNCs) were evenly mixed in a polymer matrix followed by *in situ* polymerisation under applied magnetic fields to form asymmetric hydrogel materials.[120]

5. Applications

5.1. Biomedical applications

Flexible and stretchable devices have many applications in biomedicine. This section mainly discusses the recently reported work on the actuation of flexible devices in biomedical applications, including fluid delivery,[36,53,58,200] particle and cell manipulation and separation,[201,202] and tissue engineering.[203–213]

Pneumatically actuated on-chip microvalves and micropumps are essential for efficient and accurate fluid delivery in biomedical analyses.[51,61] Zhong *et al.*[214] developed diaphragm microvalves and micropumps for automated and parallel DNA solid-phase extraction from various biological samples to eliminate cross-contamination and leakages. In addition, Lee *et al.*[51,52,59,60,62,200,215] have developed microfluidic platforms for automated, synchronous, and multiple sample analysis for various biological tests utilising on-chip microvalves and micropumps. Vo *et al.*[53] reported a pneumatically actuated

peristaltic micropump for blood plasma extraction. The pump operated at a flow rate of around 3.5 mL min⁻¹ under 300 kPa pneumatic pressure and 10 Hz operation frequency. The separation efficiency of blood plasma was 97% for a diluted sample. The advantage of this method is the elimination of external pumps. Shin et al.[216] developed a stretchable air filter for adaptive respiratory protection. They used a stretchable elastomer fibre membrane as the air filter layer where micropores of the filter were adjusted using pneumatic control, Fig. 6A. The filter characteristics were changed according to the

air quality and physical activity performed by the wearer via a machine learning algorithm. This work eliminates possible physiological and psychological effects caused by conventional respirators under dynamic environmental conditions.

Mechanical strain-based actuation was used for a strain-tuneable crack and wrinkle microvalve that can screen particles in the range of 2–20 μm.[47] These valves can screen and perform selective transport of biological cells. Mechanical strain actuation was innovatively applied in an inertial microfluidic device to adjust the cell separation cut-
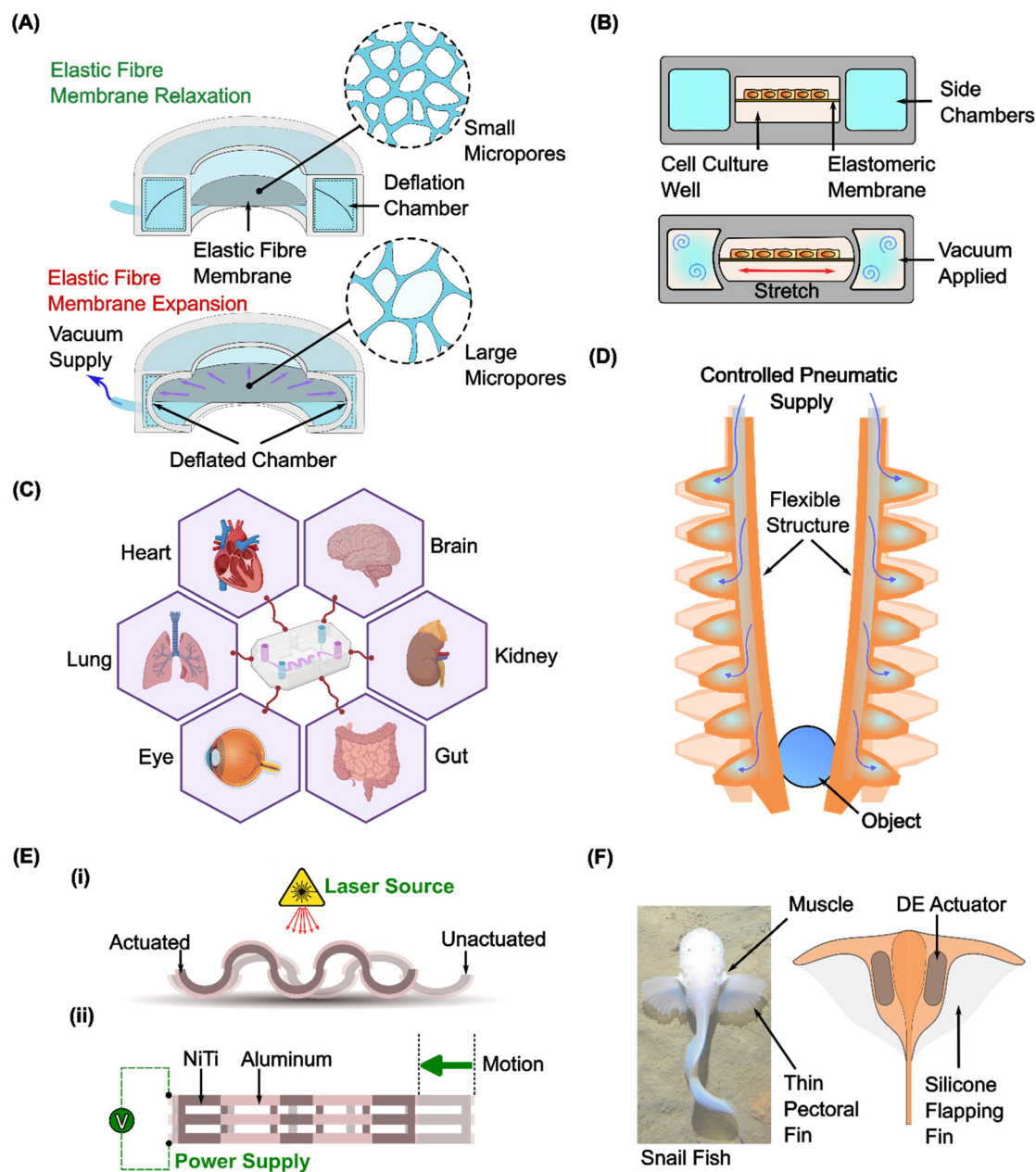

Fig. 6 Applications of flexible and stretchable actuators. (A) Dynamic pore modulation of stretchable elastic fibre membrane for adaptive respiratory protection.[216] (B) Vacuum-assisted cell-stretching device.[205] (C) Current applications of organ on a chip,[222] created with **https://BioRender.com**. (D) Soft robotic gripper operated through controlled pneumatic supply to grasp objects.[223] (E) Multiresponsive inchworm-type microrobot:[83] (i) untethered actuation through a laser source for remote operation, (ii) tethered actuation through joule heating for fast operation; (F) bio-inspired swimming robot operated through dielectric elastomer (DE) actuators.[224]

off size for the isolation of cancer cells from blood samples.[201,202] Besides, mechanical stretching was used to modify the dimension of microtrappers in real-time and on-site for the on-demand deterministic release of single cells.[217] Recently, mechanical stretching has been employed to regulate an ultra-stretchable viscoelastic microfluidic device for size-tunable sorting of *Haematococcus pluvialis*.[218]

Cell stretching is a tissue engineering technique that stretches cells and tissues to study biological functions *in vitro*.[205] The strain is associated with human body functions such as breathing, blood flow in vessels, intestinal movements, muscle contraction, *etc.*[203] In addition, cell stretching is also used to enhance medical diagnosis,[219] detecting cell morphological changes for early diagnosis of diseases.[220] Cell stretching devices have been developed to analyse the biological functions of cells under mechanical stretching.[221] These devices allow independent control of the magnitude, direction, and frequency of the mechanical strain. Moreover, biocompatible materials such as PDMS and hydrogels are widely used in cell-stretching devices where the cells can grow. Actuating mechanisms based on pneumatic, Fig. 6B, magnetic, and electromagnetic have been utilised to induce mechanical strain of these devices.[204]

Organ-on-a-chip (OoCs) is an emerging technology where tissue engineering is combined with microfluidics to mimic tissue-specific functions and to mimic key aspects of human physiology.[210] The flexible membranes located in OoCs can be actuated to mimic organ tissue motions, Fig. 6C. Huh *et al.*[207] developed a lung-on-a-chip reconstituting critical functions of the alveolar-capillary interface of the human lung. In their work, the cells adhered to a PDMS membrane were cyclically stretched and released using a vacuum source to exert physiologically relevant mechanical forces. This process allowed studies of the effect of stretching forces on physiological and pathological lung functions. In addition, Kamei *et al.*[61] developed an integrated heart/cancer-on-a-chip that uses pneumatically actuated microvalves. Here, the device performed both valving and peristaltic pumping to deliver samples. The results verified the recapitulation of the side effects and the cardiotoxicity of anti-cancer drugs *in vitro*.

5.2. Soft robotics

Soft robotics is a branch of robotics, where the components of the robots are fully or partially manufactured by mechanically compliant materials.[225] Soft robots are primarily inspired by the behaviour and structures of living organisms.[76,107,226–229] Moreover, a comprehensive study on bioinspired materials for soft robotics can be found in the recent work reported by Roh *et al.*[230] Soft robotics enables safer interactions in collaborative tasks and adaptability to unpredictable environments. Flexible and stretchable materials and suitable actuation mechanisms are paramount in soft robotics.[231,232] The actuation should provide the intended dexterity to achieve motions such as extension, contraction, twisting, and bending.[232] Actuation mechanisms

such as fluid-driven,[68,233,234] thermal,[72,88] electrical,[225,235,236] and magnetic[113,237,238] have been widely used for soft robotics. In addition, chemical actuation[239] was also applied in tactile soft robotics. The recent works highlighted the application of programmable surfaces,[111] grippers,[113,117,233] and shape-morphing structures[118] in soft robotics. More importantly, combustion-powered soft actuators shift the capabilities of mobile microrobots into a new dimension.[147]

Fluid-driven actuation is frequently applied in soft robotics, where a liquid flow[70] or compressed air[233,240] is used as the working medium, Fig. 6D. However, one significant limitation of fluid-driven actuation is the requirement for external reservoirs and pressure sources to activate the device, making the whole soft robotic system too complex and bulky. Recent studies addressed the above limitation by operating the soft robotic systems through untethered actuation sources,[68,234] designed as a part of the soft robotic device with a pre-filled actuating medium. Mechanically compliant structures made from flexible materials were used to store the working fluid, transferring the chemical energy to mechanical deformation to perform actuation tasks.

In addition, thermal actuation has been used in soft robotics where the actuator structures can be heated in untethered,[83] Fig. 6E(i), or tethered Fig. 6E(ii)[72] manners. Tethered actuation results from the deformations of the actuator material by joule heating. Untethered actuation works with incident thermal radiation *via* sources such as lasers that locally heat the actuator materials. Thermally actuated soft robots have a lower actuation speed[88] compared to their fluid-driven counterparts.

Moreover, mechanical strain-based actuation has been found in soft robotics, where highly stretchable materials such as dielectric elastomers[241] responsive to electric fields were used as the actuator structures.[136] The dielectric elastomer actuators operate under a high voltage in the kilovoltage range. For example, Li *et al.*[224] developed a deep-sea swimming soft robot using dielectric elastomer muscle actuators where pre-stretched muscles facilitated the flapping motion, Fig. 6F. The soft robot swam at a speed of 2.76 cm s^{-1} under 110 MPa when a 7 kV actuation voltage was applied at a 1 Hz frequency.

Furthermore, magnetic actuation plays a vital role in soft robotic actuation, benefiting from untethered operation and the ability to compact the structures that are difficult to achieve in other actuation principles. Magnetic soft materials are critical for soft magnetic actuators.[238] For example, McDonald *et al.*[113] developed a magnetorheological fluid-embedded elastomeric material soft actuator for multi-degree-of-freedom soft robotic applications, where they could achieve untethered and localised deformations. Moreover, Ren *et al.*[37] reported a magnetic composite elastomer-based jellyfish-inspired millirobot, which was actuated by oscillating magnetic fields.

Chemical fuel-based combustion technology has shown promising performance in mobile robotics because of the

high energy densities compared to other actuation mechanisms. Most actuation mechanisms face one or more limitations regarding energy densities, manufacturability, and scaling laws hindering the miniaturisation capabilities. Chemical combustion-based microactuation facilitates unwavering opportunities to address those drawbacks in micro-mobile robotics. A pioneering work reported a lightweight, high-frequency, power-dense microactuator operated through the combustion of methane and oxygen mixture.[143] The microactuator showed a power-to-weight ratio of 277.2 kW kg^{-1} per stroke and can produce forces over 9 N and an operating frequency above 100 Hz.

6. Discussion and future perspectives

In this review paper, we first discussed five actuation mechanisms for flexible and stretchable microdevices: fluid-driven, electro-thermal, magnetic, mechanical strain-based, and chemical. We elaborated the design parameters and performance related to each actuation concept. After that, we discussed device materials and fabrication technologies for flexible devices and actuators. Finally, we summarised the main applications of flexible and stretchable microactuators in biomedicine and soft robotics. Although the actuation for flexible microdevices has been extensively studied and significant progress has been made, there are still some challenges and limitations regarding the system complexity, device materials, and fabrication that need to be tackled to unravel the full potential of the devices.

One of the main challenges of actuation on a small scale is the bulky size and complexity of the overall system. Compact actuation schemes are necessary on the microscale to reduce system complexity. For example, the working fluids and pumping pressure for hydraulic and pneumatic microactuators are often externally supplied, and the electrothermal actuators use tethered power sources, making the whole system complicated and less portable. To eliminate these issues, self-containing working fluids and untethered power sources are promising solutions. A few pioneering works have been reported to develop a micro hydraulic actuator where the working fluid can be stored within the device[68] and an untethered thermal actuation with materials locally heated by an incident laser.[83] Besides, chemical combustion methods can achieve untethered, high-force, and rapid-response actuators. However, quantifying actuator forces remains a challenge due to the complex and dynamic nature of the combustion process, and further work is needed to understand the dynamics process of combustion and its interaction with microdevices during actuation. Moreover, the safety of chemical combustion actuation is another issue since it involves high temperature and pressure in a dynamic and chemically hazardous environment. Also, enhancing the reusability and recyclability of this actuation mechanism rather than single usage will maximise the lifespan and reduce the usage costs of devices.

Another limitation in developing flexible and stretchable devices is the material for fabricating devices. The device materials should have the required flexibility and stretchability without premature failure while in operation. PDMS has been the prominent material for microfluidic devices over the last 20 years. However, PDMS has limited stretchability (maximum strain ~120%)[157] and is prone to rupture at a high strain. Therefore, flexible materials with higher stretchability are needed. Thus, commercial silicone elastomers and thermoplastic elastomers such as Ecoflex™ and Flexdym™ have been used in flexible microdevices. These flexible materials have a much better stretchability with maximum strains of 700–900%.[156,163] However, these materials cannot be covalently bonded through plasma treatment as that of PDMS. The device fabrication techniques developed based on PDMS cannot be directly translated into these materials, and this drawback constrains their wide application in microdevices with microscale channels and ducts. Therefore, additional endeavours should be directed towards utilising these materials in the fabrication of microdevices.

Traditional flexible and stretchable microfluidic devices are fabricated mainly by the soft lithography process, where the devices are prone to fail due to the high risk of bonding failure in the layer-by-layer stacking approach, resulting in liquid leakages. Using sacrificial mould manufacturing techniques to develop intricate microdevices eliminates drawbacks associated with the multi-layer fabrication process. However, using 3D printing to manufacture sacrificial moulds has limited material availability for sacrificial moulds, minimum achievable feature size, and poor surface morphology.[242] To address this issue, 3D printing methods such as direct ink writing and stereolithography can be used to print flexible microdevices directly without sacrificial moulds. In this case, the printing resolution and development of advanced resins with good stretchability after curing are critical. UV-curable resins are emerging for highly stretchable structure fabrications. Patel et al.[243] reported a highly stretchable UV-curable elastomer with Young's modulus ranging from 0.58 to 4.21 MPa and maximum strain up to 1100%. This resin was formulated by combining epoxy aliphatic acrylate and a difunctional cross-linker of aliphatic urethane diacrylate diluted with isobornyl acrylate. Altering the ratios of epoxy aliphatic acrylate and aliphatic urethane diacrylate could tune the mechanical properties of the UV-cured elastomers. Implementing these advanced resins in high-resolution 3D printing techniques such as two-photon polymerisation (2PP) will be a promising method to print the devices directly with precise microscale features. The fabrication cost and printing efficacy of the 3D printing techniques should be optimised so that the fabrication techniques become competitive enough and easy to access for wide usage as that of PDMS fabrication.

In conclusion, as microdevices evolve from being portable to becoming wearable, there is a rising interest in flexible and stretchable devices capable of surmounting dimensional limitations, enhancing adaptability to intricate body surfaces,

and sustaining prolonged performance. Ensuring adequate actuation mechanisms becomes crucial for the optimal functionality of such devices. Selecting suitable materials and implementing precise fabrication techniques emerge as pivotal factors for the successful development and widespread adoption of these devices. Addressing current challenges related to system complexity, device materials, and fabrication techniques requires sustained and substantial efforts to advance actuation technologies for flexible microdevices.

List of abbreviations

2D	Two-dimensional
2PP	Two-photon polymerisation
3D	Three-dimensional
4D	Four-dimensional
ABS	Acrylonitrile butadiene styrene
AgNW	Silver nanowire
AMFs	Alternating magnetic fields
Bio-SHARPE	Bioinspired soft and high aspect ratio pumping element
CTE–poly(PEGDMA)	Cellulose nanocrystals assembled poly(ethylene glycol)dimethacrylate
CNCs	Cellulose nanocrystals
CNTs	Carbon nanotubes
CTE	Coefficient of thermal expansion
DE	Dielectric elastomer
DEA	Dielectric elastomer actuator
DIW	Direct-ink-writing
DNA	Deoxyribonucleic acid
EGaIn	Eutectic GaIn
EM	Electromagnetic
ESCARGOT	Embedded scaffold removing open technology
FDM	Fused deposition modeling
GO	Graphene oxide
ICP	Inductively coupled plasma
LDPE	Low density polyethylene
LIG	Laser-induced graphene
MEMS	Microelectromechanical systems
MGO	MXene graphene oxide
MR	Magnetorheological
MSMM	Magnetic shape memory material
NiTiNOL	Nickel–titanium naval ordnance laboratory
OoC	Organ-on-a-chip
PCB	Polydimethylsiloxane encapsulated carbon black
PDMS	Polydimethylsiloxane
PEGDMA	Poly(ethylene glycol)dimethacrylate
PI	Polyimide
PLA	Polylactic acid
PMMA	Polymethylmethacrylate
PNIPAm	Poly(N-isopropyl acrylamide)
PVC	Polyvinyl chloride
PVDF	Poly(vinylidene fluoride)
PZT	Lead zirconate titanate
RBCs	Red blood cells
SCHAM	Self-contained hydraulically-actuated microfluidic
SE	Silicone elastomer
SLA	Stereolithography
SMA	Shape memory alloy
SMM	Shape memory material
SMP	Shape memory polymer
SOI	Silicon-on-insulator
SOIMUMP	Silicon-on-insulator multi-user micromachining process
TCNCs	Tunicate cellulose nanocrystals
TPE	Thermoplastic elastomer
TPU	Thermoplastic polyurethane
UV	Ultraviolet
VRS	Vinylsilane-rich silicone

Author contributions

N.-T. N. and J. Z. conceptualization, supervision, and project administration. U. R. formal analysis, writing – original draft, visualization. A. M., H. C., and S. H. visualization. J. Z. and N.-T. N. writing – review & editing. N.-T. N., and J. Z. funding acquisition. All the authors provided critical feedback and read and approved the manuscript.

Conflicts of interest

The authors have declared no conflict of interest.

Acknowledgements

References

1 C. Chitrakar, E. Hedrick, L. Adegoke and M. Ecker, *Materials*, 2022, **15**, 1664.

2 Y. Zhao and X. Huang, *Micromachines*, 2017, **8**, 69.

3 H. L. O. Júnior, R. M. Neves, F. M. Monticeli and L. Dall Agnol, *Textiles*, 2022, **2**, 582–605.

4 A. Ali, H. Shaukat, S. Bibi, W. A. Altabey, M. Noori and S. A. Kouritem, *Energy Strategy Rev.*, 2023, **49**, 101124.

5 T. Meister, K. Ishida, C. Carta, N. Münzenrieder and F. Ellinger, *IEEE Microw. Mag.*, 2022, **23**, 24–44.

6 J. H. Kim, S. E. Lee and B. H. Kim, *Soft Sci.*, 2023, **3**, 16.

7 B. Inamuddin, A. Rajender and M. Abdullah, *Actuators: Fundamentals, Principles, Materials and Applications*, Wiley-Scrivener, Hoboken, NJ, 1st edn, 2020.

8 M. Zupan, M. F. Ashby and N. A. Fleck, *Adv. Eng. Mater.*, 2002, **4**, 933–940.

9 A. J. Collins, *US Pat.*, US8070094B2, 2011.

10 E. Brassitos and N. Jalili, *J. Mech. Robot.*, 2017, **9**, 061002.

11 F. H. Gern, in *Encyclopedia of Vibration*, ed. S. Braun, Elsevier, Oxford, 2001, pp. 565–577.

12 F. Larsson, *Evaluation of Aircraft Actuator Technologies*, Linköping University Electronic Press, Linköping, 2023, vol. 1955.

13 S. D. Oehler, D. J. Hartl, R. Lopez, R. J. Malak and D. C. Lagoudas, *Smart Mater. Struct.*, 2012, **21**, 094016.

14 D. J. Hartl, D. C. Lagoudas, F. T. Calkins and J. H. Mabe, *Smart Mater. Struct.*, 2009, **19**, 015020.

15 S. Wang, Z. Weng and B. Jin, *Appl. Sci.*, 2020, **10**, 4352.

16 M. Feidt, in *Finite Physical Dimensions Optimal Thermodynamics 1*, ed. M. Feidt, Elsevier, 2017, pp. 99–124.

17 S. T. Smith and R. M. Seugling, *Precis. Eng.*, 2006, **30**, 245–264.

18 A. Barbot, F. Ortiz, A. Bolopion, M. Gauthier and P. Lambert, *Annu. Rev. Control Robot. Auton. Syst.*, 2023, **6**, 313–334.

19 B. Sahu, C. R. Taylor and K. K. Leang, *J. Manuf. Sci. Eng.*, 2010, **132**, 1–16.

20 Y. Wu, C. Liu, M. Lapiere, J. L. Ciatti, D. S. Yang, J. Berkovich, J. B. Model, A. Banks, R. Ghaffari, J.-K. Chang, R. G. Nuzzo and J. A. Rogers, *Adv. Mater. Technol.*, 2023, **8**, 2300732.

21 M. J. Ansari, R. R. Rajendran, S. Mohanto, U. Agarwal, K. Panda, K. Dhotre, R. Manne, A. Deepak, A. Zafar, M. Yasir and S. Pramanik, *Gels*, 2022, **8**, 454.

22 I. Miranda, A. Souza, P. Sousa, J. Ribeiro, E. M. S. Castanheira, R. Lima and G. Minas, *J. Funct. Biomater.*, 2021, **13**, 2.

23 L. Peponi, I. Navarro-Baena and J. M. Kenny, in *Smart Polymers and their Applications*, ed. M. R. Aguilar and J. San Román, Woodhead Publishing, 2014, pp. 204–236.

24 L. Lin and C.-K. Chung, *Micromachines*, 2021, **12**, 1350.

25 A.-I. Bunea, N. del Castillo Iniesta, A. Droumpali, A. E. Wetzel, E. Engay and R. Taboryski, *Micro*, 2021, **1**, 164–180.

26 A. Cowen, G. Hames, D. Monk, S. Wilcenski and B. Hardy, *SOIMUMPs Design Handbook*, Memscap Inc., Durham, NC, USA, 2011, vol. 6.

27 V. Saggiomo and A. H. Velders, *Adv. Sci.*, 2015, **2**, 1500125.

28 B. J. Nelson, I. K. Kaliakatsos and J. J. Abbott, *Annu. Rev. Biomed. Eng.*, 2010, **12**, 55–85.

29 M. Li, A. Pal, A. Aghakhani, A. Pena-Francesch and M. Sitti, *Nat. Rev. Mater.*, 2022, **7**, 235–249.

30 H. Fischer, B. Vogel and A. Welle, *Minim. Invasive Ther. Allied Technol.*, 2004, **13**, 248–253.

31 B. Yan, *Micromachines*, 2022, **13**, 1756.

32 G.-H. Lee, H. Moon, H. Kim, G. H. Lee, W. Kwon, S. Yoo, D. Myung, S. H. Yun, Z. Bao and S. K. Hahn, *Nat. Rev. Mater.*, 2020, **5**, 149–165.

33 C. Zhang, D. Xing and Y. Li, *Biotechnol. Adv.*, 2007, **25**, 483–514.

34 H. Fallahi, J. Zhang, H.-P. Phan and N.-T. Nguyen, *Micromachines*, 2019, **10**, 830.

35 N.-T. Nguyen, *Micromachines*, 2020, **11**, 1004.

36 J. Davies, M. T. Thai, H. Low, P. T. Phan, T. T. Hoang, N. H. Lovell and T. N. Do, *Soft Robot.*, 2023, **10**, 1055–1069.

37 Z. Ren, W. Hu, X. Dong and M. Sitti, *Nat. Commun.*, 2019, **10**, 2703.

38 M. Runciman, A. Darzi and G. P. Mylonas, *Soft Robot.*, 2019, **6**, 423–443.

39 G. M. Whitesides, *Angew. Chem., Int. Ed.*, 2018, **57**, 4258–4273.

40 P. Wang, M. Hu, H. Wang, Z. Chen, Y. Feng, J. Wang, W. Ling and Y. Huang, *Adv. Sci.*, 2020, **7**, 2001116.

41 X. Liu, H. Song, W. Zuo, G. Ye, S. Jin, L. Wang and S. Li, *Energies*, 2022, **15**, 8731.

42 M. O. Tariq, S. A. Bazaz, J. Ahmed and M. M. Saleem, *IEEE Sens. J.*, 2022, **22**, 22438–22445.

43 J. Huang, X. Zhang, R. Liu, Y. Ding and D. Guo, *Nat. Commun.*, 2023, **14**, 1483.

44 Y. He, J. Tang, Y. Hu, S. Yang, F. Xu, M. Zrínyi and Y. Mei Chen, *Chem. Eng. J.*, 2023, **462**, 142193.

45 J. Zuo, H. Chen, J. Gu, W. Zhang, Z. Zhang and G. Huang, *Sens. Actuators, A*, 2023, **352**, 114208.

46 N. Bao, Q. Liu, M. F. Reynolds, M. Figueras, E. Smith, W. Wang, M. C. Cao, D. A. Muller, M. Mavrikakis, I. Cohen, P. L. McEuen and N. L. Abbott, *Proc. Natl. Acad. Sci. U. S. A.*, 2023, **120**, e2221740120.

47 Y. Liu, M. Cheng, J. Huang, Y. Liu, Y. Chen, Y. Xiao, S. Chen, X. Ouyang, H. Cheng and X. Wang, *ACS Appl. Mater. Interfaces*, 2021, **13**, 36849–36858.

48 V. De and D. Reynaerts, *J. Micromech. Microeng.*, 2010, **20**, 043001.

49 C.-W. Huang, S.-B. Huang and G.-B. Lee, *J. Micromech. Microeng.*, 2006, **16**, 2265.

50 J. Cui and T. Pan, *J. Micromech. Microeng.*, 2011, **21**, 065034.

51 P. Gopinathan, A. Sinha, Y.-D. Chung, S.-C. Shiesh and G.-B. Lee, *Analyst*, 2019, **144**, 4943–4951.

52 R. Gandotra, T.-W. Chen, F.-C. Kuo, M. S. Lee and G.-B. Lee, *Biosens. Bioelectron.*, 2023, **229**, 115120.

53 T. N. A. Vo, P.-C. Chen, P.-S. Chen and W.-H. Liu, *Sens. Actuators, A*, 2023, **358**, 114430.

54 S. A. M. Shaegh, A. Pourmand, M. Nabavinia, H. Avci, A. Tamayol, P. Mostafalu, H. B. Ghavifekr, E. N. Aghdam, M. R. Dokmeci, A. Khademhosseini and Y. S. Zhang, *Sens. Actuators, B*, 2018, **255**, 100–109.

55 G. Yamauchi and T. Ishida, *Sens. Actuators, A*, 2021, **332**, 113082.

56 S. Shibamoto, W. Lu and A. Sato, *J. Chromatogr. A*, 2023, **1696**, 463961.

57 F. Shao, K. Hsieh, P. Zhang, A. M. Kaushik and T.-H. Wang, *Sci. Rep.*, 2022, **12**, 13340.

58 A. Tsiamis, A. Buchoux, S. T. Mahon, A. J. Walton, S. Smith, D. J. Clarke and A. A. Stokes, *Micromachines*, 2023, **14**, 537.

59 A. Sinha, P. Gopinathan, Y.-D. Chung, S.-C. Shiesh and G.-B. Lee, *Lab Chip*, 2019, **19**, 1676–1685.

60 A. Sinha, P. Gopinathan, Y.-D. Chung, H.-Y. Lin, K.-H. Li, H.-P. Ma, P.-C. Huang, S.-C. Shiesh and G.-B. Lee, *Biosens. Bioelectron.*, 2018, **122**, 104–112.

61 K.-I. Kamei, Y. Kato, Y. Hirai, S. Ito, J. Satoh, A. Oka, T. Tsuchiya, Y. Chen and O. Tabata, *RSC Adv.*, 2017, **7**, 36777–36786.

62 P. Gopinathan, L.-Y. Hung, C.-H. Wang, N.-J. Chiang, Y.-C. Wang, Y.-S. Shan and G.-B. Lee, *Biomicrofluidics*, 2017, **11**, 044101.

63 Y. Zhou, Z. Yu, M. Wu, Y. Lan, C. Jia and J. Zhao, *Talanta*, 2023, **253**, 124044.

64 C. Chen, P. Li, T. Guo, S. Chen, D. Xu and H. Chen, *Biosensors*, 2022, **12**, 868.

65 S.-C. Huang, G.-B. Lee, F.-C. Chien, S.-J. Chen, W.-J. Chen and M.-C. Yang, *J. Micromech. Microeng.*, 2006, **16**, 1251.

66 R. Zengerle, J. Ulrich, S. Kluge, M. Richter and A. Richter, *Sens. Actuators, A*, 1995, **50**, 81–86.

67 N. C. Speller, G. G. Morbioli, M. E. Cato, J. L. McNeice and A. M. Stockton, *Sens. Actuators, B*, 2020, **303**, 127124.

68 G. L. Smith, J. B. Tyler, N. Lazarus, H. Tsang, L. Viornery, J. Shultz and S. Bergbreiter, *Adv. Funct. Mater.*, 2023, **33**, 2207435.

69 Y. Cheng, K. H. Chan, X.-Q. Wang, T. Ding, T. Li, X. Lu and G. W. Ho, *ACS Nano*, 2019, **13**, 13176–13184.

70 H. Yuk, S. Lin, C. Ma, M. Takaffoli, N. X. Fang and X. Zhao, *Nat. Commun.*, 2017, **8**, 14230.

71 J. Kedzierski and H. Chea, *Microsyst. Nanoeng.*, 2021, **7**, 22.

72 Z. Zhang, F. Bu, E. Cheng, C. Yang, Z. Zhang and N. Hu, *Adv. Eng. Mater.*, 2023, **25**, 2300253.

73 P. Won, K. K. Kim, H. Kim, J. J. Park, I. Ha, J. Shin, J. Jung, H. Cho, J. Kwon, H. Lee and S. H. Ko, *Adv. Mater.*, 2021, **33**, 2002397.

74 H. Kim, H. Lee, I. Ha, J. Jung, P. Won, H. Cho, J. Yeo, S. Hong, S. Han, J. Kwon, K.-J. Cho and S. H. Ko, *Adv. Funct. Mater.*, 2018, **28**, 1801847.

75 U. Roshan, R. Amarasinghe and N. Dayananda, *J. Robot. Netw. Artif. Life*, 2018, **5**, 194–198.

76 Y. Yoon, H. Park, J. Lee, J. Choi, Y. Jung, S. Han, I. Ha and S. H. Ko, *Chem. Eng. J.*, 2023, **451**, 138794.

77 Y. Ling, W. Pang, X. Li, S. Goswami, Z. Xu, D. Stroman, Y. Liu, Q. Fei, Y. Xu, G. Zhao, B. Sun, J. Xie, G. Huang, Y. Zhang and Z. Yan, *Adv. Mater.*, 2020, **32**, 1908475.

78 R. Hickey, M. Kujath and T. Hubbard, *J. Vac. Sci. Technol., A*, 2002, **20**, 971–974.

79 R.-C. Voicu and C. Tibeica, *Micromachines*, 2023, **14**, 797.

80 M. Teymoori and Ö. Kocatürk, *Smart Mater. Struct.*, 2022, **31**, 065025.

81 S. Ahn, W. Jung, K. Ko, Y. Lee, C. Lee and Y. Hwang, *Micromachines*, 2021, **12**, 46.

82 S. Timoshenko, *J. Opt. Soc. Am.*, 1925, **11**, 233–255.

83 X. Hui, J. Luo, R. Wang and H. Sun, *ACS Nano*, 2023, **17**, 6589–6600.

84 Z. Liu, R. Zhang, K. Yang, Y. Yue, F. Wang, K. Li, G. Wang, J. Lian and G. Xin, *ACS Appl. Mater. Interfaces*, 2022, **14**, 39031–39038.

85 M. Hashimoto, T. Sato and Y. Taguchi, *Sens. Actuators, A*, 2023, **356**, 114348.

86 H. Lee, H. Kim, I. Ha, J. Jung, P. Won, H. Cho, J. Yeo, S. Hong, S. Han, J. Kwon, K.-J. Cho and S. H. Ko, *Soft Robot.*, 2019, **6**, 760–767.

87 X. Hui, J. Luo, X. Wang, R. Wang and H. Sun, *Appl. Phys. Lett.*, 2022, **121**, 023502.

88 H. Wang, Z. Zhao, P. Liu, Y. Pan and X. Guo, *ACS Appl. Mater. Interfaces*, 2022, **14**, 41283–41295.

89 H. Guckel, J. Klein, T. Christenson, K. Skrobis, M. Laudon and E. G. Lovell, in *Technical Digest IEEE Solid-State Sensor and Actuator Workshop*, 1992, pp. 73–75.

90 C. S. Pan and W. Hsu, *J. Micromech. Microeng.*, 1997, **7**, 7–13.

91 J. H. Comtois and V. M. Bright, *Sens. Actuators, A*, 1997, **58**, 19–25.

92 T. Moulton and G. K. Ananthasuresh, *Sens. Actuators, A*, 2001, **90**, 38–48.

93 M. Akbari, F. Barazandeh and H. Barati, *Sens. Actuators, A*, 2022, **346**, 113877.

94 M. Kaur and C. Menon, *Sensors*, 2023, **23**, 404.

95 M. Lara-Castro, A. Herrera-Amaya, M. A. Escarola-Rosas, M. Vázquez-Toledo, F. López-Huerta, L. A. Aguilera-Cortés and A. L. Herrera-May, *Micromachines*, 2017, **8**, 203.

96 J. Zhang, H. Wu, H. Shen, L. Xue, W. Zhang, Y. Liu, F. Du, L. Pan, H. Huang, L. Lin and L. Chen, *Sens. Actuators, A*, 2022, **341**, 113579.

97 L. Que, J.-S. Park and Y. B. Gianchandani, *J. Microelectromech. Syst.*, 2001, **10**, 247–254.

98 Y. B. Gianchandani and K. Najafi, *J. Microelectromech. Syst.*, 1996, **5**, 52–58.

99 E. T. Enikov, S. S. Kedar and K. V. Lazarov, *J. Microelectromech. Syst.*, 2005, **14**, 788–798.

100 M. Tecpoyotl-Torres, P. Vargas-Chable, J. Escobedo-Alatorre, L. Cisneros-Villalobos and J. Sarabia-Vergara, *Micromachines*, 2022, **13**, 1460.

101 J. Dai, Y. Bu, J. Xie, K. Li, Z. Xiong, B. Tang, Q. Tao and M. Gao, *J. Microelectromech. Syst.*, 2021, **30**, 622–631.

102 K. T. Hoang, D. T. Nguyen and P. H. Pham, *Microsyst. Technol.*, 2020, **26**, 1479–1487.

103 T. Sciberras, M. Demicoli, I. Grech, B. Mallia, P. Mollicone and N. Sammut, *Micromachines*, 2023, **14**, 1264.

104 M. Pustan, R. Chiorean, C. Birleanu, C. Dudescu, R. Muller, A. Baracu and R. Voicu, *Microsyst. Technol.*, 2017, **23**, 3863–3871.

105 J. Mohd Jani, M. Leary, A. Subic and M. A. Gibson, *Mater. Des.*, 2014, **56**, 1078–1113.

106 B. T. Chia, H.-H. Liao and Y.-J. Yang, *Sens. Actuators, A*, 2011, **165**, 86–93.

107 J. Lee, Y. Yoon, H. Park, J. Choi, Y. Jung, S. H. Ko and W.-H. Yeo, *Adv. Intell. Syst.*, 2022, **4**, 2100271.

108 J.-H. Kim, K.-H. Na, C. J. Kang and Y.-S. Kim, *Sens. Actuators, A*, 2005, **120**, 365–369.

109 J. R. Brauer, *Magnetic Actuators And Sensors*, Wiley-IEEE Press, 2nd edn, 2014.

110 D. P. Arnold and N. Wang, *J. Microelectromech. Syst.*, 2009, **18**, 1255–1266.

111 X. Ni, H. Luan, J.-T. Kim, S. I. Rogge, Y. Bai, J. W. Kwak, S. Liu, D. S. Yang, S. Li, S. Li, Z. Li, Y. Zhang, C. Wu, X. Ni, Y. Huang, H. Wang and J. A. Rogers, *Nat. Commun.*, 2022, **13**, 5576.

112 M. Dehghan and M. Tahmasebipour, *J. Micromech. Microeng.*, 2023, **33**, 075005.

113 K. McDonald, A. Rendos, S. Woodman, K. A. Brown and T. Ranzani, *Adv. Intell. Syst.*, 2020, **2**, 2000139.

114 K. Ullakko, L. Wendell, A. Smith, P. Müllner and G. Hampikian, *Smart Mater. Struct.*, 2012, **21**, 115020.

115 E. Quandt and A. Ludwig, *Sens. Actuators, A*, 2000, **81**, 275–280.

116 X. Liu, W. Zuo, H. Song, T. Shang, H. Dong, L. Wang, J. Shao and S. Li, *Energies*, 2022, **15**, 8094.

117 J. E. Lee, Y. Sun, Y.-C. Sun, I. R. Manchester and H. E. Naguib, *Appl. Mater. Today*, 2022, **29**, 101681.

118 J. Tang, Q. Yin, Y. Qiao and T. Wang, *ACS Appl. Mater. Interfaces*, 2019, **11**, 21194–21200.

119 A. R. Smith, A. Saren, J. Järvinen and K. Ullakko, *Microfluid. Nanofluid.*, 2015, **18**, 1255–1263.

120 C. Gong, Y. Zhai, J. Zhou, Y. Wang and C. Chang, *J. Mater. Chem. C*, 2022, **10**, 549–556.

121 Y. Yang, Z. He, G. Lin, H. Wang and P. Jiao, *Int. J. Mech. Sci.*, 2022, **229**, 107513.

122 S. Ganguly and S. Margel, *Polymer*, 2021, **13**, 4259.

123 A. E. Deatsch and B. A. Evans, *J. Magn. Magn. Mater.*, 2014, **354**, 163–172.

124 A. Saren, A. R. Smith and K. Ullakko, *Microfluid. Nanofluid.*, 2018, **22**, 38.

125 L. Seigner, G. K. Tshikwand, F. Wendler and M. Kohl, *Actuators*, 2021, **10**, 181.

126 S.-H. Song, J.-Y. Lee, H. Rodrigue, I.-S. Choi, Y. J. Kang and S.-H. Ahn, *Sci. Rep.*, 2016, **6**, 21118.

127 W. Pang, X. Cheng, H. Zhao, X. Guo, Z. Ji, G. Li, Y. Liang, Z. Xue, H. Song, F. Zhang, Z. Xu, L. Sang, W. Huang, T. Li and Y. Zhang, *Natl. Sci. Rev.*, 2020, **7**, 342–354.

128 X. Ning, X. Yu, H. Wang, R. Sun, R. E. Corman, H. Li, C. M. Lee, Y. Xue, A. Chempakasseril, Y. Yao, Z. Zhang, H. Luan, Z. Wang, W. Xia, X. Feng, R. H. Ewoldt, Y. Huang, Y. Zhang and J. A. Rogers, *Sci. Adv.*, 2018, **4**, eaat8313.

129 R. Pelrine, R. Kornbluh, Q. Pei and J. Joseph, *Science*, 2000, **287**, 836–839.

130 Z. Liu, Y. D. Liu, Q. Shi and Y. Liang, *J. Mater. Sci.*, 2021, **56**, 14943–14963.

131 M. Kohl, M. Gueltig, V. Pinneker, R. Yin, F. Wendler and B. Krevet, *Micromachines*, 2014, **5**, 1135–1160.

132 M. Kabla, E. Ben-David and D. Shilo, *Smart Mater. Struct.*, 2016, **25**, 075020.

133 Y. Kotb, I. Elgamal and M. Serry, *Micromachines*, 2021, **12**, 520.

134 S. Seelecke, J. Neu, S. Croce, J. Hubertus, G. Schultes and G. Rizzello, *Actuators*, 2023, **12**, 141.

135 Z. Chen, Y. Xiao, J. Fang, J. He, Y. Gao, J. Zhao, X. Gao and Y. Luo, *Chem. Eng. J.*, 2021, **405**, 126634.

136 Y. Guo, L. Liu, Y. Liu and J. Leng, *Adv. Intell. Syst.*, 2021, **3**, 2000282.

137 J. Huang, F. Wang, L. Ma, Z. Zhang, E. Meng, C. Zeng, H. Zhang and D. Guo, *Chem. Eng. J.*, 2022, **428**, 131354.

138 A. P. Gerratt, B. Balakrisnan, I. Penskiy and S. Bergbreiter, *Smart Mater. Struct.*, 2014, **23**, 055004.

139 X. Che, M. Wu, G. Yu, C. Liu, H. Xu, B. Li and C. Li, *Chem. Eng. J.*, 2022, **433**, 133672.

140 J. Yi, G. Zou, J. Huang, X. Ren, Q. Tian, Q. Yu, P. Wang, Y. Yuan, W. Tang, C. Wang, L. Liang, Z. Cao, Y. Li, M. Yu, Y. Jiang, F. Zhang, X. Yang, W. Li, X. Wang, Y. Luo, X. J. Loh, G. Li, B. Hu, Z. Liu, H. Gao and X. Chen, *Nature*, 2023, **624**, 295–302.

141 M. Wang, L. Zhou, W. Deng, Y. Hou, W. He, L. Yu, H. Sun, L. Ren and X. Hou, *ACS Nano*, 2022, **16**, 2672–2681.

142 Y. Aishan, Y. Yalikun, Y. Shen, Y. Yuan, S. Amaya, T. Okutaki, A. Osaki, S. Maeda and Y. Tanaka, *Sens. Actuators, B*, 2021, **337**, 129769.

143 C. A. Aubin, R. H. Heisser, O. Peretz, J. Timko, J. Lo, E. F. Helbling, S. Sobhani, A. D. Gat and R. F. Shepherd, *Science*, 2023, **381**, 1212–1217.

144 W. Ge, F. Zhang, D. Wang, Q. Wei, Q. Li, Z. Feng, S. Feng, X. Xue, G. Qing and Y. Liu, *Small*, 2022, **18**, 2107105.

145 G. Jia, A. Zheng, X. Wang, L. Zhang, L. Li, C. Li, Y. Zhang and L. Cao, *Sens. Actuators, B*, 2021, **346**, 130507.

146 R. F. Shepherd, A. A. Stokes, J. Freake, J. Barber, P. W. Snyder, A. D. Mazzeo, L. Cademartiri, S. A. Morin and G. M. Whitesides, *Angew. Chem., Int. Ed.*, 2013, **52**, 2892–2896.

147 R. L. Truby, *Science*, 2023, **381**, 1152–1153.

148 R. H. Heisser, C. A. Aubin, O. Peretz, N. Kincaid, H. S. An, E. M. Fisher, S. Sobhani, P. Pepiot, A. D. Gat and R. F. Shepherd, *Proc. Natl. Acad. Sci. U. S. A.*, 2021, **118**, e2106553118.

149 Y. Yang, B. Hou, J. Chen, H. Wang, P. Jiao and Z. He, *Extreme Mech. Lett.*, 2020, **37**, 100731.

150 D. C. Duffy, J. C. McDonald, O. J. A. Schueller and G. M. Whitesides, *Anal. Chem.*, 1998, **70**, 4974–4984.

151 A. J. T. Teo, F. Malekpour-galogahi, K. R. Sreejith, T. Takei and N.-T. Nguyen, *AIP Adv.*, 2020, **10**, 065101.

152 S. H. Tan, N.-T. Nguyen, Y. C. Chua and T. G. Kang, *Biomicrofluidics*, 2010, **4**, 032204.

153 H. Nakano, S. Kakinoki and Y. Iwasaki, *Colloids Surf., B*, 2021, **205**, 111900.

154 M. W. Toepke and D. J. Beebe, *Lab Chip*, 2006, **6**, 1484–1486.

155 J. N. Lee, C. Park and G. M. Whitesides, *Anal. Chem.*, 2003, **75**, 6544–6554.

156 J. Vaicekauskaite, P. Mazurek, S. Vudayagiri and A. L. Skov, *J. Mater. Chem. C*, 2020, **8**, 1273–1279.

157 I. D. Johnston, D. K. McCluskey, C. K. L. Tan and M. C. Tracey, *J. Micromech. Microeng.*, 2014, **24**, 035017.

158 K. Song, N.-K. Cho, K. Park and C.-S. Kim, *Polymer*, 2022, **14**, 2373.

159 S. Zhang, C. Ge and R. Liu, *Sens. Actuators, A*, 2022, **341**, 113580.

160 *Ecoflex™ Series*, Super-Soft, Addition Cure Silicone Rubbers, **https://www.smooth-on.com/product-line/ecoflex/**, (accessed October 13, 2023).

161 *Dragon Skin™ Series*, High Performance Silicone Rubber, **https://www.smooth-on.com/product-line/dragon-skin/**, (accessed October 13, 2023).

162 Y. Hao, T. Wang, Z. Ren, Z. Gong, H. Wang, X. Yang, S. Guan and L. Wen, *Int. J. Adv. Robot. Syst.*, 2017, **14**, 1729881417707148.

163 J. Lachaux, C. Alcaine, B. Gómez-Escoda, C. M. Perrault, D. O. Duplan, P.-Y. J. Wu, I. Ochoa, L. Fernandez, O.

Mercier, D. Coudreuse and E. Roy, *Lab Chip*, 2017, **17**, 2581–2594.

164 M. S. Xavier, C. D. Tawk, Y. K. Yong and A. J. Fleming, *Sens. Actuators, A*, 2021, **332**, 113199.

165 X. Xu, Y. Liu, W. Fu, M. Yao, Z. Ding, J. Xuan, D. Li, S. Wang, Y. Xia and M. Cao, *Polymer*, 2020, **12**, 580.

166 A. K. Mishra, T. J. Wallin, W. Pan, A. Xu, K. Wang, E. P. Giannelis, B. Mazzolai and R. F. Shepherd, *Sci. Robot.*, 2020, **5**, eaaz3918.

167 X. M. Ma, R. Li, J. Ren, X. C. Lv, X. H. Zhao, Q. Ji and Y. Z. Xia, *RSC Adv.*, 2017, **7**, 47767–47774.

168 Y. Wang, X. Ma, Y. Jiang, W. Zang, P. Cao, M. Tian, N. Ning and L. Zhang, *Resour. Chem. Mater.*, 2022, **1**, 308–324.

169 L. J. Romasanta, M. A. Lopez-Manchado and R. Verdejo, *Prog. Polym. Sci.*, 2015, **51**, 188–211.

170 S. Mohammadpourfazeli, S. Arash, A. Ansari, S. Yang, K. Mallick and R. Bagherzadeh, *RSC Adv.*, 2023, **13**, 370–387.

171 W. Zhang, G. Wu, H. Zeng, Z. Li, W. Wu, H. Jiang, W. Zhang, R. Wu, Y. Huang and Z. Lei, *Polymer*, 2023, **15**, 2766.

172 D. Won, H. Cho, H. Kim, G. Lee, J. Kwon, J. Kim, S. Hong, J. Choi, S.-W. Kim and S. H. Ko, *Adv. Opt. Mater.*, 2022, **10**, 2201206.

173 H. Lu, Z. Li, X. Qi, L. Xu, Z. Chi, D. Duan, M. Z. Islam, W. Wang, X. Jin, Y. Zhu, Y. Fu, L. Cui, Y. Zhuang and Y. Dong, *Compos. Sci. Technol.*, 2021, **207**, 108697.

174 F. M. Vivaldi, A. Dallinger, A. Bonini, N. Poma, L. Sembranti, D. Biagini, P. Salvo, F. Greco and F. Di Francesco, *ACS Appl. Mater. Interfaces*, 2021, **13**, 30245–30260.

175 M. Kim, B.-U. Moon and C. H. Hidrovo, *J. Micromech. Microeng.*, 2013, **23**, 095024.

176 T. Nguyen and M. Khine, *Polymer*, 2020, **12**, 1454.

177 Z. Liao, J. Yang, M. Hossain, G. Chagnon, L. Jing and X. Yao, *Int. J. Mech. Sci.*, 2021, **206**, 106624.

178 D. J. Case, Y. Liu, I. Z. Kiss, J.-R. Angilella and A. E. Motter, *Nature*, 2019, **574**, 647–652.

179 *Flexdym Pellets - Polymer for Mass Production*, https://eden-microfluidics.com/eden-materials/flexdym-pellets-microfluidics-for-mass-production/, (accessed August 3, 2023).

180 H. J. Qi and M. C. Boyce, *Mech. Mater.*, 2005, **37**, 817–839.

181 C. Qu, J. Hu, X. Liu, Z. Li and Y. Ding, *Materials*, 2017, **10**, 1329.

182 I. Ghosh, J. Konar and A. K. Bhowmick, *J. Adhes. Sci. Technol.*, 1997, **11**, 877–893.

183 F. Van Loock and N. A. Fleck, *Polymer*, 2018, **148**, 259–268.

184 M. S. Zafar, *Polymer*, 2020, **12**, 2299.

185 Y. Jin, T. Yang, S. Ju, H. Zhang, T.-Y. Choi and A. Neogi, *Polymer*, 2020, **12**, 1462.

186 K. Haraguchi, H.-J. Li, Y. Xu and G. Li, *Polymer*, 2016, **96**, 94–103.

187 C. Greiner, S. M. Oppenheimer and D. C. Dunand, *Acta Biomater.*, 2005, **1**, 705–716.

188 P. Poornima Vijayan, in *Shape Memory Polymers, Blends and Composites: Advances and Applications*, ed. J. Parameswaranpillai, S. Siengchin, J. J. George and S. Jose, Springer, Singapore, 2020, pp. 199–217.

189 O. Niwa, M. Kakuchi and T. Tamamura, *Polym. J.*, 1987, **19**, 1293–1301.

190 C.-W. Chiang and E.-Y. Chuang, *Int. J. Nanomed.*, 2019, **14**, 1575–1585.

191 S. Afrin, M. Shahruzzaman, P. Haque, M. S. Islam, S. Hossain, T. U. Rashid, T. Ahmed, M. Takafuji and M. M. Rahman, *Gels*, 2022, **8**, 340.

192 C. G. Willson and M. D. Stewart, in *Encyclopedia of Materials: Science and Technology*, ed. K. H. J. Buschow, R. W. Cahn, M. C. Flemings, B. Ilschner, E. J. Kramer, S. Mahajan and P. Veyssière, Elsevier, Oxford, 2001, pp. 6973–6977.

193 J. A. Walker, K. J. Gabriel and M. Mehregany, *Sens. Actuators, A*, 1990, **21**, 243–246.

194 T. D. Ngo, A. Kashani, G. Imbalzano, K. T. Q. Nguyen and D. Hui, *Composites, Part B*, 2018, **143**, 172–196.

195 D. Han and H. Lee, *Curr. Opin. Chem. Eng.*, 2020, **28**, 158–166.

196 F. Daniel, J. Fontenot and A. D. Radadia, *Sens. Actuators, A*, 2022, **333**, 113302.

197 B. Jian, H. Li, X. He, R. Wang, H. Y. Yang and Q. Ge, *Int. J. Extreme Manuf.*, 2023, **6**, 012001.

198 F. Momeni, S. M. Mehdi Hassani, N. X. Liu and J. Ni, *Mater. Des.*, 2017, **122**, 42–79.

199 Q. Ge, C. K. Dunn, H. J. Qi and M. L. Dunn, *Smart Mater. Struct.*, 2014, **23**, 094007.

200 H.-B. Wu, C.-H. Wang, Y.-D. Chung, Y.-S. Shan, Y.-J. Lin, H.-P. Tsai and G.-B. Lee, *Anal. Chim. Acta*, 2023, **1274**, 341531.

201 H. Fallahi, S. Yadav, H.-P. Phan, H. Ta, J. Zhang and N.-T. Nguyen, *Lab Chip*, 2021, **21**, 2008–2018.

202 H. Fallahi, J. Zhang, J. Nicholls, H.-P. Phan and N.-T. Nguyen, *Anal. Chem.*, 2020, **92**, 12473–12480.

203 D. Y. M. Leung, S. Glagov and M. B. Mathews, *Exp. Cell Res.*, 1977, **109**, 285–298.

204 W. Zhang, G. Huang and F. Xu, *Front. Bioeng. Biotechnol.*, 2020, **8**, 589590.

205 I. Constantinou and E. E. Bastounis, *Trends Biotechnol.*, 2023, **41**, 939–950.

206 L. Wu, Y. Ai, R. Xie, J. Xiong, Y. Wang and Q. Liang, *Lab Chip*, 2023, **23**, 1192–1212.

207 D. Huh, B. D. Matthews, A. Mammoto, M. Montoya-Zavala, H. Y. Hsin and D. E. Ingber, *Science*, 2010, **328**, 1662–1668.

208 Y. Zhao, E. Y. Wang, F. B. L. Lai, K. Cheung and M. Radisic, *Trends Biotechnol.*, 2023, **41**, 410–424.

209 J. Ko, D. Park, S. Lee, B. Gumuscu and N. L. Jeon, *Micromachines*, 2022, **13**, 1200.

210 C. M. Leung, P. de Haan, K. Ronaldson-Bouchard, G.-A. Kim, J. Ko, H. S. Rho, Z. Chen, P. Habibovic, N. L. Jeon, S. Takayama, M. L. Shuler, G. Vunjak-Novakovic, O. Frey, E. Verpoorte and Y.-C. Toh, *Nat. Rev. Methods Primers*, 2022, **2**, 1–29.

211 Q. Wu, J. Liu, X. Wang, L. Feng, J. Wu, X. Zhu, W. Wen and X. Gong, *J. Geophys. Res. Planets*, 2020, **19**, 9.

212 K. Ronaldson-Bouchard and G. Vunjak-Novakovic, *Cell Stem Cell*, 2018, **22**, 310–324.

213 D. P. Thomas, J. Zhang, N.-T. Nguyen and H. T. Ta, *Biosensors*, 2023, **13**, 136.

214 R. Zhong, M. Wang and B. Lin, *Electrophoresis*, 2023, **44**, 825–834.

215 T.-W. Chen, R. Gandotra, H.-Y. Chang, M. S. Lee, F.-C. Kuo and G.-B. Lee, *Anal. Chem.*, 2023, **95**, 7693–7701.

216 J. Shin, S. Jeong, J. Kim, Y. Y. Choi, J. Choi, J. G. Lee, S. Kim, M. Kim, Y. Rho, S. Hong, J.-I. Choi, C. P. Grigoropoulos and S. H. Ko, *ACS Nano*, 2021, **15**, 15730–15740.

217 H. Fallahi, H. Cha, H. Adelnia, Y. Dai, H. Thu Ta, S. Yadav, J. Zhang and N.-T. Nguyen, *Nanoscale Horiz.*, 2022, **7**, 414–424.

218 Z. Jia, J. Wu, X. Wu, Q. Yuan, Y. Chan, B. Liu, J. Zhang and S. Yan, *Anal. Chem.*, 2023, **95**, 13338–13345.

219 S. Yadav, M. Barton and N.-T. Nguyen, *Adv. Biosyst.*, 2020, **4**, 1900222.

220 S. Yadav, R. Vadivelu, M. Ahmed, M. Barton and N.-T. Nguyen, *Exp. Cell Res.*, 2019, **378**, 191–197.

221 S. Yadav, P. Singha, N.-K. Nguyen, C. H. Ooi, N. Kashaninejad and N.-T. Nguyen, *Micromachines*, 2023, **14**, 1537.

222 D. Park, J. Lim, J. Y. Park and S.-H. Lee, *Stem Cells Transl. Med.*, 2015, **4**, 1352–1368.

223 S. Zhuo, Z. Zhao, Z. Xie, Y. Hao, Y. Xu, T. Zhao, H. Li, E. M. Knubben, L. Wen, L. Jiang and M. Liu, *Sci. Adv.*, 2020, **6**, eaax1464.

224 G. Li, X. Chen, F. Zhou, Y. Liang, Y. Xiao, X. Cao, Z. Zhang, M. Zhang, B. Wu, S. Yin, Y. Xu, H. Fan, Z. Chen, W. Song, W. Yang, B. Pan, J. Hou, W. Zou, S. He, X. Yang, G. Mao, Z. Jia, H. Zhou, T. Li, S. Qu, Z. Xu, Z. Huang, Y. Luo, T. Xie, J. Gu, S. Zhu and W. Yang, *Nature*, 2021, **591**, 66–71.

225 M. W. M. Tan, G. Thangavel and P. S. Lee, *Adv. Funct. Mater.*, 2021, **31**, 2103097.

226 S. Coyle, C. Majidi, P. LeDuc and K. J. Hsia, *Extreme Mech. Lett.*, 2018, **22**, 51–59.

227 S. Dodampegama, A. Mudugamuwa, M. Konara, N. Perera, D. De Silva, U. Roshan, R. Amarasinghe, N. Jayaweera and H. Tamura, *Appl. Sci.*, 2022, **12**, 11542.

228 P. Won, S. H. Ko, C. Majidi, A. W. Feinberg and V. A. Webster-Wood, *Actuators*, 2020, **9**, 96.

229 Z. Xie, F. Yuan, J. Liu, L. Tian, B. Chen, Z. Fu, S. Mao, T. Jin, Y. Wang, X. He, G. Wang, Y. Mo, X. Ding, Y. Zhang, C. Laschi and L. Wen, *Sci. Robot.*, 2023, **8**, eadh7852.

230 Y. Roh, Y. Lee, D. Lim, D. Gong, S. Hwang, M. Kang, D. Kim, J. Cho, G. Kwon, D. Kang, S. Han and S. H. Ko, *Adv. Funct. Mater.*, 2023, 2306079.

231 X. Zhou and W. Cao, *Nanomaterials*, 2023, **13**, 316.

232 L. Hines, K. Petersen, G. Z. Lum and M. Sitti, *Adv. Mater.*, 2017, **29**, 1603483.

233 J. Walker, T. Zidek, C. Harbel, S. Yoon, F. S. Strickland, S. Kumar and M. Shin, *Actuators*, 2020, **9**, 3.

234 Y. Yang, Y. Xie, J. Liu, P. Jiang and Y. Chen, *J. Intell. Robot. Syst.*, 2023, **108**, 16.

235 M. Franke, A. Ehrenhofer, S. Lahiri, E.-F. M. Henke, T. Wallmersperger and A. Richter, *Front. Robot. AI*, 2020, **7**, 510757.

236 Z. Ma and D. Sameoto, *Micromachines*, 2022, **13**, 1881.

237 H. Wang, Z. Zhu, H. Jin, R. Wei, L. Bi and W. Zhang, *J. Alloys Compd.*, 2022, **922**, 166219.

238 Y. Kim and X. Zhao, *Chem. Rev.*, 2022, **122**, 5317–5364.

239 Z. Zheng, H. Wang, L. Dong, Q. Shi, J. Li, T. Sun, Q. Huang and T. Fukuda, *Nat. Commun.*, 2021, **12**, 411.

240 Q. Song, Y. Chen, P. Hou, P. Zhu, D. Helmer, F. Kotz-Helmer and B. E. Rapp, *Micromachines*, 2023, **14**, 244.

241 J.-H. Youn, S. M. Jeong, G. Hwang, H. Kim, K. Hyeon, J. Park and K.-U. Kyung, *Appl. Sci.*, 2020, **10**, 640.

242 S. Poornaganti, S. N. Yeole and J. P. Kode, *Mater. Today: Proc.*, 2022, **62**, 3837–3848.

243 D. K. Patel, A. H. Sakhaei, M. Layani, B. Zhang, Q. Ge and S. Magdassi, *Adv. Mater.*, 2017, **29**, 1606000.